Arthritis Research & Therapy

RESEARCH

Open Access

Low dose methotrexate impaired T cell transmigration through down-regulating CXCR4 expression in rheumatoid arthritis (RA)

Lei Ding[1], Daniel H. Park[2], Bo Gao[1,3], Lingyuan Wu[4], Meizhang Li[5], Haitham Abedelhakim[6*] and Ming Zhang[7*]

Abstract

Background CXC chemokine CXCL12 is involved in the pathological development of rheumatoid arthritis (RA) through abnormal migration of peripheral immune cells in the joint. Although low dose methotrexate (MTX) is clinically used to treat RA patients, CXCL12 signaling responses to MTX-mediated treatments is still not well understood.

Methods In this study, we examined the expression of CXCR4 (cognatic receptor for CXCL12) in peripheral T cells from RA patients and arthritis mice models received from low dose MTX therapies. The effects of low dose MTX on CXCR4 were further determined via both in vitro $CD3^+$ T cells and *Cxcr4* conditional knockout (CKO) arthritis mice models.

Results Our clinical data shows that low dose MTX treatment was clinically associated with down-regulated expression of chemokine receptor CXCR4 on patient peripheral T cells. In vitro, low dose MTX significantly decreased cell transmigration through down-regulated CXCR4's expression in $CD3^+$ T cells. Consistently, $CD3^+$ T cells treated with low dose MTX demonstrated an increased genomic hypermethylation across the promoter region of *Cxcr4* gene. Furthermore, our preclinical studies showed that low dose MTX-mediated downregulation of CXCR4 significantly improved the pathological development in mouse arthritis models. Conditional disruption of the *Cxcr4* gene in peripheral immune cells potentially alleviated inflammation of joints and lung tissue in the arthritis mice, though genetic modification itself overall did not change their clinical scores of arthritis, except for a significant improvement on day 45 in CXCR4 CKO arthritis mice models during the recovery phase.

Conclusion Our findings suggest that the effect of low dose MTX treatment could serve to eliminate inflammation in RA patients through impairment of immune cell transmigration mediated by CXCR4.

Keywords Rheumatoid arthritis, Methotrexate, Chemokine, CXCR4, Conditional knockout

*Correspondence:
Haitham Abedelhakim
habdelhakim@kumc.edu
Ming Zhang
zhangming99@gmail.com
[1]School of Life Sciences, Yunnan University, Kunming, Yunnan 650091, China
[2]Pediatric Emergency Medicine, Johns Hopkins University, Baltimore, MD 21218, USA
[3]College of Bioengineering, Sichuan University of Science and Engineering, Yibin, Sichuan 644000, China
[4]Emory University School of Medicine, Atlanta, GA 30322, USA
[5]Department of Pathology and Laboratory Medicine, University of Kansas Medical Center, Kansas City, KS 66103, USA
[6]Division of Hematologic Malignancies and Cellular Therapeutics, University of Kansas Medical Center, 3901 Rainbow Blvd. 4019 Wahl Hall East, MS 3040, Kansas City, KS 66103, USA
[7]Institute of Neuroscience, Kunming Medical University, 931 Basic Medical Blvd. 1168 Chunrong West Road, Kunming, Yunnan 650500, China

Introduction

Rheumatoid arthritis (RA) is a complex autoimmune disorder characterized by chronic inflammation of joint synovia and progressive destruction of cartilage and bone [1]. The pathological development of RA is directly related to the abnormal infiltration of T and B lymphocytes, neutrophils, monocytes, and macrophages into synovial tissues, joints, and other organs [2, 3]. It has been widely accepted that infiltrated cells mainly rely on chemokines and their cognate receptors to functionally mediate their migration from circulation to the organs [4–6]. However, targeting chemokine signaling has failed to show clinical improvements though RA-related animal models. On the other hand, agents that target chemokines (receptors) have yielded some promising results [7]. Even so, persistent accumulation of lymphocytic cells within the synovial compartment strongly supports that either chemokines or chemokine receptors play significant roles during the pathological development of RA.

CXC motif chemokine ligand 12 (SDF-1/CXCL12) and its receptor CXC motif chemokine receptor 4 (CXCR4) comprise an important chemotaxis involving both immune response and brain development [8]. In RA patients, it was found that CXCL12 enhanced the accumulation of CXCR4-expressing $CD4^+$, $CD8^+$, and Th1 cells within their synovium [9–12]. Others suggested that synovial TGF-beta 1 (TGFB1) also played an important role to induce CXCR4's protein expression on $CD4^+$ T cells [11]. Besides lymphocytes, Lenoir et al. (2004) reported that CXCL12 regulated desensitization of human neutrophil respiratory burst in patient synovial fluid [13]. More importantly, some preclinical studies already showed that targeting CXCR4 with the specific inhibitor AMD3100 resulted in efficient decrease of RA-associated pathogenesis in collagen-induced arthritis (CIA) mice [14, 15]. In the same manner, Chung et al. (2010) reported that the incidence of CIA was significantly reduced in $Cxcr4^{flox/flox}$/Lck-Cre mice compared with $Cxcr4^{+/+}$/Lck-Cre mice [16]. These findings indicate that CXCL12-CXCR4 is an important chemotaxis responsible for the abnormal migration of peripheral lymphocytes to the arthritis synovium during the pathological development of RA patients.

As an analog of folic acid, methotrexate (4-amino-10-methylfolic acid, MTX) was originally designed as anticancer medication, given as high as 1 gram in a single dose [17]. High-dose methotrexate antagonized the folate pathway by inhibiting dihydrofolate reductase (DHFR) and purine synthesis, thus leading cancer cells to their apoptotic fate [18]. Low dose MTX (7.5–25 mg weekly) currently serves as one of the most popular first line medications to treat RA patients [19]. However, low-dose MTX may involve more complex molecular mechanisms than folate antagonism in the treatment of RA patients [18, 20–22]. Indeed, it has been reported that MTX decreased the expression of inflammatory factors such as tumor necrosis factor alpha (TNF-α), interleukin 1 beta (IL-1β), interleukin 6 (IL-6), interleukin 8 (IL-8), C-C motif chemokine ligand 5 (RANTES/CCL5), chemokine (CXC motif) ligand 1 (GRO/CXCL1), and adhesion molecules in RA patients [23–28]. Although the presence of upregulated plasma CXCL12 has been suggested in RA patients, the effect of MTX on this chemokine currently remains controversial [29, 30]. In psoriatic patients, immunohistochemical studies in the skin biopsies suggested that decreased CXCL12 was associated with high dose MTX treatment [31]. In RA patients' synovial tissue, decreased C-C motif chemokine ligand 2 (MCP-1/CCL2) protein has been suggested to be associated with the clinical MTX treatment [24]. Barsig et al. (2005) also reported that MTX was able to significantly suppress cytokine and chemokine release in inflamed joints in a dose-dependent fashion in an adjuvant arthritis-associated rat model [32]. Other studies suggested that MTX potentially enhanced the receptor interleukin 17 receptor A (IL-17R) expression [33] but decreased interleukin 1 receptor type 1 (IL-1r) expression [27]. Some studies showed that inflammatory arthritis is usually associated with global DNA hypomethylation in peripheral blood mononuclear cells (PBMCs), which could be reverted with MTX treatment in inflammatory arthritis [34–36].

In the current study, although enhanced CXCR4 expression on peripheral immune cells was observed in RA patients, we report that CXCR4's expression was decreased after different clinical treatments. The effects of low dose MTX on CXCR4's expression and functions were further determined. Our study discloses the mechanism by which MTX depends on to target peripheral lymphocytes during treatment of RA patients. These findings thus shed light on potential roles of CXCR4 on peripheral immune cells that were involved in the pathological development of RA.

Materials and methods

Clinical samples

Forty-eight patients with clinically active RA were diagnosed through fulfillment of the 1987 American College of Rheumatology criteria [37] and were recruited from the outpatient clinic of the Rheumatology department of First Affiliated Hospital of Kunming Medical University of Yunnan Province. Written informed consent for the present study's use of human peripheral blood was obtained from all forty-eight patients and thirty-seven healthy donors, and ethical approval was obtained from both the Ethics Committee of the First Affiliated Hospital of Kunming Medical University and the Committee on Human Subject Research and Ethics

of Yunnan University (Approved number: 20190801). All experiments were carried out according to the relevant guidelines.

Cell sorting and cell culture

For the isolation of PBMCs, the heparinized whole blood samples (4 mL) from each RA patient and healthy donor were diluted with an equal volume of PBS (Biosharp Life Sciences, China), layered onto Ficoll-Hypaque (Solarbio Life Sciences, China) and centrifuged at 2,000 rpm/min, at 20 °C for 20 min by density gradient centrifugation. Mononuclear cells were recovered from the interface and washed twice with PBS. The $CD3^+$ T cells were purified from about $2–10\times10^8$ PBMCs, which were passaged over a 30 μm nylon wool column, incubated using immunomagnetic microbeads (Miltenyi Biotec, Germany) for 30 min at 4 °C, and finally selected with QuadroMACS™ Separator (Miltenyi Biotec, Germany) via magnetic LS cell separation columns (Miltenyi Biotec, Germany). All assays were performed according to the protocols recommended by the manufacturer. Aliquots of $4–10\times10^6$ PBMCs and purified $CD3^+$ T cells were optionally stimulated with anti-CD3 (clone UCHT1, 2.5 μg/ml) and anti-CD28 (clone CD28.2, 1.25 μg/ml) antibodies (BD Bioscience, USA) for 48 h in the presence of MTX does (0.001–1 μg/mL or 0.01 μg/mL) or AMD3100 (1 μg/mL) in vitro. Jurkat cells were offered by Professor Shenghong Li from the Insititute of Botany, the Chinese Academy of Sciences, Kunming, China. The PBMCs, purified $CD3^+$ T cells and Jurkat cells were cultured in flat-bottom plates (Corning, USA) in RPMI-1640 medium (Gibco, Invitrogen Corporation, USA) supplemented with 10% fetal calf serum (Viva Cell Biosciences, China), 100 U/mL penicillin and 100 μg/mL streptomycin (BasalMedia Technologies, China) at 37 °C under 5% CO_2.

Flow cytometry (FCM)

Expression of chemokine receptor CXCR4 on human T cells was analyzed using flow cytometry. 100 μL of human PBMCs (about 5×10^5 cells) were incubated with mouse anti-human antibodies, including anti-CD184-PE and anti-CD3-FITC (20 μL, BD Biosciences, USA), anti- CD4- and CD8-FITC (5 μL, BioLegend, USA), and their corresponding mouse isotypes as the negative controls. Then, the cells were incubated for 30 min at 4 °C in the dark. Subsequently, the cells were washed twice with 1 mL FACS buffer (1% BSA in PBS) by centrifugation (400 g/min, 5 minutes, 4 °C) to remove unbound antibodies. Cells were then resuspended in 500 μL PBS and sieved through a 40-μm pore size mesh to generate single-cell suspensions. Finally, labeled cells were measured on an Accuri C6 Flow Cytometer (Accuri Cytometers, BD Biosciences, C6, USA) and analyzed by FlowJo software (Treestar FlowJo v10.8.1, Ashland, USA). Negative fluorescence was gated with FITC-conjugated IgG or PE-conjugated IgG. At least 10,000 events collected within the lymphocyte gate. The single fluorochrome-stained cells were used for instrument compensation and the photomultiplier tube (PMT) setup. Analysis of $CD3^+$, $CD4^+$, $CD8^+$ T cell subsets were performed on the total $CD3^+$ T cells within the lymphocyte gate.

Quantitative real-time polymerase chain reaction (qRT-PCR)

Total messenger RNA (mRNA) was extracted using RNAiso Plus Reagent (Clontech Laboratories, Takara Bio Group, Japan) according to the manufacturer's instructions. Potential genomic DNA contamination was removed from the samples and complement DNA (cDNA) was synthesized from 1 μg total RNA per sample using random primers with PrimeScript™ RT reagent Kit with gDNA Eraser (Clontech Laboratories, Takara Bio Group, Japan) according to the recommended protocol. The qRT-PCR with up to 100 ng cDNA was amplified using the SYBR® Premix Ex Taq™ (Tli RNaseH Plus, Clontech Laboratories, Takara Bio Group, Japan). The ABI Prism 7500 Sequence Detection System (Applied Biosystems, ABI 7500, USA) was used to measure the amplified PCR product. The qRT-PCR thermal cycle included 1 cycle of 95 °C for 10 s, followed by a two-step PCR program: 40 cycles of 95 °C for 5 s, and 60 °C for 34 s, followed by a melt curve analysis. Each sample was performed in triplicate (technical replicates) and repeated at least three times independently. The oligonucleotide primers used for qRT-PCR analyses were listed in Table S2. The relative expression of qRT-PCR data was determined using the $2^{-\Delta\Delta Ct}$ method to compare mRNA expression levels of the target gene with the housekeeping gene (β-actin or 18 S).

CXCR4 methylation-specific PCR analysis based on nucleotide sequencing

The Jurkat cells, or the 0.01 μg/mL MTX treated $CD3^+$ T cells, genomic DNA was extracted by DNA mini isolation kits (Qiagen, Germany) according to the manufacturer's protocol. Genomic DNA was bisulfite converted with the Zymo EZ DNA methylation kits (Zymo Research, Irvine, CA, USA), and the CpG sites of the bisulfite modified DNA were amplified with bisulfite specific PCR consisted of an initial denaturation step at 95 °C for 5 min, followed by 38 cycles of denaturation at 95 °C for 30 s, annealing at 54 °C for 30 s, extension at 72 °C for 30 s, and final extension step at 72 °C for 7 min by the EpiArt HS Taq Master Mix (Vazyme Biotech, Nanjing, China). The PCR products were verified on 2% agarose gel, followed with sequencing by Sangon Biotech Co., Ltd. (Shanghai, China). For each CpG site, the methylation ratio was calculated as the number of cytosine reads divided

by the sum of cytosine and thymine reads [38]. Bisulfite PCR primer sequences were designed by Methyl Primer Express Software v1.0 (Applied Biosystems, USA) and listed in Table S2.

In vitro transmigration

The interaction between CXCR4 and extracellular matrix (ECM, Sigma-Aldrich, USA) assays were conducted on sorting cells with 0.01 μg/mL MTX (Sigma-Aldrich, USA) and CXCR4-specific antagonist 1 μg/mL AMD3100 (Sigma-Aldrich, USA) treatment, using NeuroProbe 48-Well Micro Chemotaxis Chambers (Neuro Probe, Inc. Ap48, USA). Briefly, the Chemotaxis Chambers were separated using 5 μm pore polycarbonate transwell filter membranes (Neuro Probe, Inc. USA) and the lower side was coated with 0.01 mg/mL ECM diluted with RPMI-1640 culture media. In the lower wells, the 100 ng/mL human CXCL12 (SDF-1α) protein (Miltenyi Biotec, Germany) was supplemented as the chemoattractant. And then, 1×10^4 mock or pre-treated cells suspended in 50 μL RPMI-1640 culture media were added into each upper chamber. After 4 hours of incubation at 37 °C and 5% CO_2, the membrane was carefully removed. Cells on the upper membrane surface were gently scraped with a cotton swab. The membranes were fixed in 4% (w/v) paraformaldehyde (PFA, Servicebio Technology, China) for 30 min and washed in PBS before staining with 0.1% Hoechst 33342 (Sigma-Aldrich, USA) for 5 min at room temperature, followed by rinsing three times with PBS. The membranes were mounted on glass slides with Fluoro-Gel (Electron Microscopy Sciences, USA) and cells per unit area in triplicate were determined by counting four representative microscopic fields under an epifluorescence microscope at a magnification of ×10 (Leica, DMi8, Germany).

Cell viability assay

To examine the toxicity of low-dose MTX on the activated T cells, PBMCs were seeded into 96-well flat bottom plates and stimulated with anti-CD3 (clone UCHT1, 2.5 μg/ml) and anti-CD28 (clone CD28.2, 1.25 μg/ml) antibodies (BD Bioscience, USA) for 0, 24 and 48 h in PBS or MTX (0.001–1 μg/mL) at the density of 5×10^4 cells per well (100 μL) in quadruplicate. The same volume of PBS was kept consistent with the 0.001–1 μg/mL MTX group added in the vehicle control group for 0, 24 and 48 h, respectively. The effects of MTX on the survival of cells was evaluated with CellTiter 96® Aqueous One Solution Reagent Solution Cell Proliferation Assay kit (Promega, USA), following the manufacturer instructions. Briefly, at 2 h before each of the desired time points, each well was mixed with 20 μL of MTS ((3-(4,5-dimethylthiazol-2-yl)-5-(3-carboxymethoxyphenyl)-2-(4-sulfophenyl)-2 H-tetrazolium, solution inner salt, and cells were incubated at 37 °C with 5% CO_2 for 2 h. The absorbances of the samples were detected at a wavelength of 490 nm using a micro-plate reader (Molecular Devices, SpectraMax 190, USA).

Enzyme-linked immunosorbent assay (ELISA)

The clinical sample blood serums were collected, and enzyme-linked immunosorbent assay (ELISA) kits for detecting human cytokines IL-1, IL-2, IL-6, IL-8, TNF-α (Elsbio Biotec, China) and CXCL12 were obtained (Solarbio Life Sciences, China). ELISA experiments were conducted following the manufacturers' instructions. Plates were read by a micro-plate reader (Molecular Devices, SpectraMax 190, USA) at a wavelength of 450 nm.

In vivo MTX and AMD3100 treatment

For in vivo assessment of the effect of MTX on the treatment of RA, we used adjuvant-induced arthritis (AA) mouse models that were widely used for drug validation, in particular for T cell-related pathways leading to arthritis [39]. Briefly, thirty-two 10-week-old female C57BL/6J mice were purchased from Vital River Laboratories (Beijing, China) to be used as the experimental model of arthritis. They were kept in healthy conditions with clean air and given plenty of food and water. To avoid superimposed side effects of MTX/AMD3100 treatment and adjuvant immunization on the growth and body weight of arthritis mice, a preventative model with MTX and AMD3100 treatments began on day 1 and lasted 15 days. Briefly, the mice were divided into four groups (eight mice per group). The non-arthritic healthy control mice and untreated arthritis mice received 150 μl normal saline (NS) every three days for 15 days (5 times total) and were then divided into two groups: namely non-arthritic healthy control mice were fed normally, untreated arthritis mice were induced by intradermal tail injection with 150 μl of 4 mg/mL heat-killed *Mycobacterium tuberculosis* suspended in complete Freund's adjuvant (CFA) (day16, Sigma Aldrich, USA). The MTX or AMD3100 treatment of them established arthritis group was fed with 2.5 mg/kg MTX or 5 mg/kg AMD3100 from day 1 to day 15 every three days, and arthritis was subsequently induced with the same regimen. Mice were weighed and scored for clinical signs of arthritis once every two days from day 17 to day 48 post-immunization. On day 20, 27, and 38, blood was collected and analyzed for $CXCR4^+$PBMCs. All animal studies and relevant procedures were reviewed and approved by the ethics committee of the institutional animal care and use committee, Yunnan University (IACUC, YNU) (Approved number: 20190801).

Collagen induced arthritis (CIA) mouse model

The type II collagen induced arthritis (CIA) mouse models, which were extensively used to identify potential pathogenic mechanisms of autoimmunity, including the role of individual cell types in disease onset and progression [40], were induced and the effect of CXCR4 on the occurrence and development of RA was assessed. Briefly, 10-week-old female C57BL/6J mice were injected intradermally at the base of the tail with 15 mg/kg chicken type II collagen (CII, Chondrex, USA) dissolved in 10 mM acetic acid and emulsified in an equal volume of CFA (Sigma Aldrich, USA) containing 4 mg/mL *Mycobacterium tuberculosis* to induce the arthritis mice model (day 0). Twenty-one days (day 21) after the first primary immunization, the mice were given a single booster injection in the same manner. The arthritis index assay, blood collection, and histological assessment were carried out. The expression of TNFα, IL-1β and IL-6 in lung tissue was detected by qRT-PCR and the respective primers used were listed in Table S2.

CXCR4 conditional knockout

Mx1-Cre^{-}/CXCR4$^{flox/flox}$ mice (C57BL/6J) were purchased from the Jackson laboratory (The Jackson laboratory, USA). In these mice, two LoxP sites were genetically inserted in the side of the second exon of the *Cxcr4* gene. LoxP site was genotyped using genotyping PCR primers MG-Loxp-F and MG-Loxp-R. A 577-bp and 481-bp DNA band was expected from either flox homozygous mice or wild type/flox heterozygous mice respectively. Meanwhile, Mx1-cre^{+}/CXCR4$^{+/+}$ mice (C57BL/6J) were purchased from Nanjing Biomedical Research Institute of Nanjing University (Nanjing, China). These mice overexpressed the Cre protein under control of the inducible Mx1 promoter. Mx1-Cre^{+} was genotyped using genotyping primers MG-Cre-F and MG-Cre-R, and a 408-bp PCR DNA band was expected as well. The Mx1-Cre^{-}/CXCR4$^{flox/flox}$ mice and Mx1-Cre^{+}/CXCR4$^{+/+}$ mice were founders to be crossbred to obtain Mx1-Cre^{+}/CXCR$^{flox/flox}$ mice. To obtain CXCR4 conditional knockout mice, Mx1-Cre^{+}/CXCR4$^{flox/flox}$ mice were administrated 12.5 mg/kg polyinosinic-polycytidylic acid (PI: PC, Novus Biologicals, USA) by intraperitoneal injection. PI: PC injections were performed every two days, for a total of 3 times. Genetic deletion of *Cxcr4* allele genes was verified using genotyping primers MG-CXCR4-F and MG-CXCR4-R. CXCR4^{+}PBMCs and CXCR4^{+}CD3^{+} T cells on mouse PBMCs were confirmed by flow cytometry. All the primers used were listed in **Table S2**. The CIA mice model of *Cxcr4* conditional knockout was induced as above (Collagen induced arthritis mouse model) mentioned. In brief, 10-week-old female Mx1-Cre^{+}/Cxcr4$^{flox/flox}$ mice were immunized intradermally at the base of the tail with 15 mg/kg chicken type II collagen (CII, Chondrex, USA) dissolved in 10 mM acetic acid and emulsified in an equal volume of CFA (Sigma Aldrich, USA) containing 4 mg/mL *Mycobacterium tuberculosis* (day 0) after the PI: PC was injected at day -2, day -4, and day -6 respectively. On day 21, the mice were given a single booster injection with the same manner. The arthritis index assay, blood collection, histological assessment, and the expression of TNFα, IL-1β and IL-6 in lung tissue were carried out.

Histological assessments of arthritis

At the end of the mice experimental procedure, the knee joints and paws were analyzed for histological assessment after the mice were sacrificed. Animals were perfused with 4% phosphate-buffered paraformaldehyde (PFA). Then, animal joints, paws and lungs were removed, dissected, and sliced into 5-μm cross-sections. Sections were stained by hematoxylin and eosin (H&E) (Beyotime Life Sciences, China) according to standard procedures. The severity of arthritic changes, such as articular cartilage destruction and bone erosion were histologically scored as described previously [41]. Briefly, we scored cartilage destruction from 0 to 3 and bone erosion from 0 to 5. The positive inflammatory areas of mouse lung sections were measured on each slide and quantified using ImageJ software [42].

Statistical analysis

All reported values were expressed as mean ± SEM (Standard Error of Mean), unless otherwise stated. The arthritis mice and MTX and AMD3100 treated experimental groups included at least five mice. Statistical analyses were done with SPSS 22.0 computer software (SPSS Inc, Chicago, USA). The statistical significance between healthy controls and patient, sham and MTX treated mice, sham and arthritis mice were analyzed using unpaired Student t-test. The statistical significance between two groups of qRT-PCR, in vitro transmigration and cell viability assay were analyzed with a paired Student's t-tests. In all statistical analyses, the probability (*P*) values less than 0.05 were statistically significant.

Results

CXCR4-expressing peripheral cells was increased in RA patients

From 48 patients (Table 1) with longstanding RA, the CXCR4-expressing (CXCR4^{+}PBMCs) was analyzed by flow cytometry. As shown in the Fig. S1D and Table S1, about 12.35 ± 1.57% of CXCR4^{+}PBMCs were detected in RA patients. However, only 3.48 ± 0.25% PBMCs in the heathy control were found to express CXCR4. Similar observations were obtained when examining CXCR4's protein expression on patients' CD3^{+} T cells. About 7.11 ± 1.15% of CXCR4^{+}CD3^{+} T cells were detected in

Table 1 Summary of RA patients and healthy controls

	Healthy	RA patients
Age, yrs,	51.35 ± 4.06	52.29 ± 2.05
Male, n (%)	13(35.14%)	8(16.67%)
Female, n (%)	24(64.86%)	40(83.33)
Current Smoker, n (%)	4(10.81%)	3(6.25%)
Alcohol Drinker (n, %)	0	2(4.17%)
Weight, Kg, mean + SEM	57.97 ± 1.29	54.81 ± 1.94
BMI*, Kg/m^2, mean + SEM	21.29 ± 0.43	22.04 ± 0.67
Total, n	37	48

*Body Mass Index

RA patients, while only 1.81 ± 0.13% of CXCR4$^+$CD3$^+$ T cells were observed in the heathy control (Fig. S1C and S1E). Considering the averaged CD3$^+$ T cell (Fig. S1B and S1G) and PBMCs cell numbers (Fig. S1A and S1F) from both groups were almost the same, it was concluded that CXCR4's expression was significantly increased in the RA patients compared with the healthy controls. The results showed a significant increase in the expression of CXCR4 on PBMCs and CD3$^+$ T cells, with an averaged 3.55-fold change ($P<0.001$) and 3.93-fold change ($P<0.001$) respectively between RA patients and the healthy control. We also found that the frequency of CXCR4$^+$CD3$^+$ T cells in RA exhibited a significantly positive correlation with the patients' clinical scores of DAS28/ESR, SDAI, TJC in 28 joints, PtGA and PhGA (Fig. S2A, C, D, F, G, $P<0.05$ or 0.001), and a moderate positive correlation with DAS28/CRP (Fig. S2B, $P=0.091$) and almost no correlations with SJC in 28 joints (Fig. S2E, $P=0.423$). These results reveal that CXCR4 on CD3$^+$ T cells is an activating factor associated with RA disease activity.

The serum protein level of inflammation cytokines from RA patients was further analyzed by ELISA. Interestingly, we found that protein concentrations of cytokines IL-1, IL-2, IL-8, and TNFα were upregulated in RA compared with the healthy control (Fig. S3A-D). The protein concentration of IL-6 was increased in RA, but there was no statistical significance (Fig. S3E). Consistent with previous results [30], we observed serum chemokine CXCL12 was significantly increased by 68.40 ± 1.54% ($P=0.004$) in the RA patients as compared to the healthy control (Fig. S3F). Our results showed an increased serum level of inflammatory and pro-inflammatory factors in RA patients. These observations suggested that either CXCL12's serum level or CXCR4's expression on CD3$^+$ T cells was potentially associated with the enhanced inflammatory environment found during the pathological development of RA.

CXCR4-expressing peripheral CD3$^+$ T cells was decreased in RA patients after clinical treatments

To analyze the effects of clinical treatments on RA patients, the same 48 RA patients were further regrouped into three different subgroups (Table 2): (1) RA-Untreated (RA patients without clinical treatments, $n=9$); (2) RA + MTX (RA patients clinically treated with MTX, $n=15$); (3) RA-MTX (RA patients clinically treated without MTX, $n=24$). As shown in Fig. 1C and E, about 15.98 ± 3.42% of CXCR4$^+$CD3$^+$ T cells were detected in RA-Untreated patients. Meanwhile, 1.81 ± 0.13% of CXCR4$^+$CD3$^+$ T cells were detected from the healthy control, consistently demonstrating an 8.8-fold ($P<0.001$) increase of CXCR4's expression on CD3$^+$ T cells in RA-Untreated as compared to the healthy control. Furthermore, we noticed that only 5.67 ± 1.43% of CXCR4$^+$CD3$^+$ T cells were detected from RA-MTX patients and 4.08 ± 0.21% CXCR4$^+$CD3$^+$ T cells in RA + MTX patients. Compared to RA-Untreated patients, expression of CXCR4 on CD3$^+$ T cells decreased significantly by a 2.8-fold change ($P<0.001$) and 3.9-fold change ($P<0.001$) in RA-MTX and RA + MTX patients respectively. CXCR4$^+$PBMCs was also observed to be decreased in RA patients after different treatments (Fig. 1D). However, both CXCR4$^+$PBMCs and CXCR4$^+$CD3$^+$ T cells was not different between the RA + MTX and RA-MTX treatment groups (Fig. 1D-E). The total number of PBMCs between RA-Untreated and RA + MTX patient groups was not changed, while the total number of CD3$^+$ T cells was increased between RA-Untreated and RA + MTX patient groups (Fig. 1A-B, F-G). We further regrouped the RA-MTX group into GC monotherapy, DMARDs and biology agent, DMARDs and prednisone, DMARDs and biology agent and prednisone and others (leflunomide monotherapy, hydroxychloroquine monotherapy) groups according to their clinical treatment. We found that the proportions of CXCR4$^+$PBMCs (Fig.

Table 2 Clinical characteristics of different RA groups ($n=48$). Data are mean ± SEM

Clinical	RA-Untreated ($n=9$)	RA + MTX ($n=15$)	RA-MTX ($n=24$)
Symptom Duration, mo	62.89 ± 32.86	99.53 ± 8.97	134.92 ± 27.49
TJC in 28 joints	15.78 ± 2.29	9.07 ± 0.51	8.25 ± 1.35
SJC in 28 joints	5.33 ± 2.20	5.00 ± 0.44	4.46 ± 0.99
PtGA, cm (0–10 cm scale)	96.67 ± 1.67	52.67 ± 1.41	62.71 ± 4.18
PhGA, cm (0–10 cm scale)	81.11 ± 2.00	37.67 ± 1.29	45.00 ± 4.17
DAS28/ESR score	6.93 ± 0.34	5.15 ± 0.08	5.11 ± 0.33
DAS28/CRP score	6.09 ± 0.32	4.42 ± 0.09	4.59 ± 0.31
SDAI score	40.01 ± 7.09	21.03 ± 0.89	21.40 ± 2.49
ESR, mm/h	54.67 ± 14.67	36.47 ± 1.35	39.50 ± 5.85
CRP, mg/L	42.51 ± 12.20	16.94 ± 1.75	23.81 ± 4.99

Note RA patient were diagnosed according to the clinical diagnostic standards that meet the criteria from the 1987 American College of Rheumatology [37], and the disease activity was assessed using the European League Against Rheumatism (EULAR) criteria (See the details in the Supplemental Materials and methods). Patient group included RA-Untreated (RA patients without clinical treatments), RA + MTX (RA patients treated with low dose MTX), RA-MTX (RA patients treated without low dose MTX). Data represented as mean ± SEM

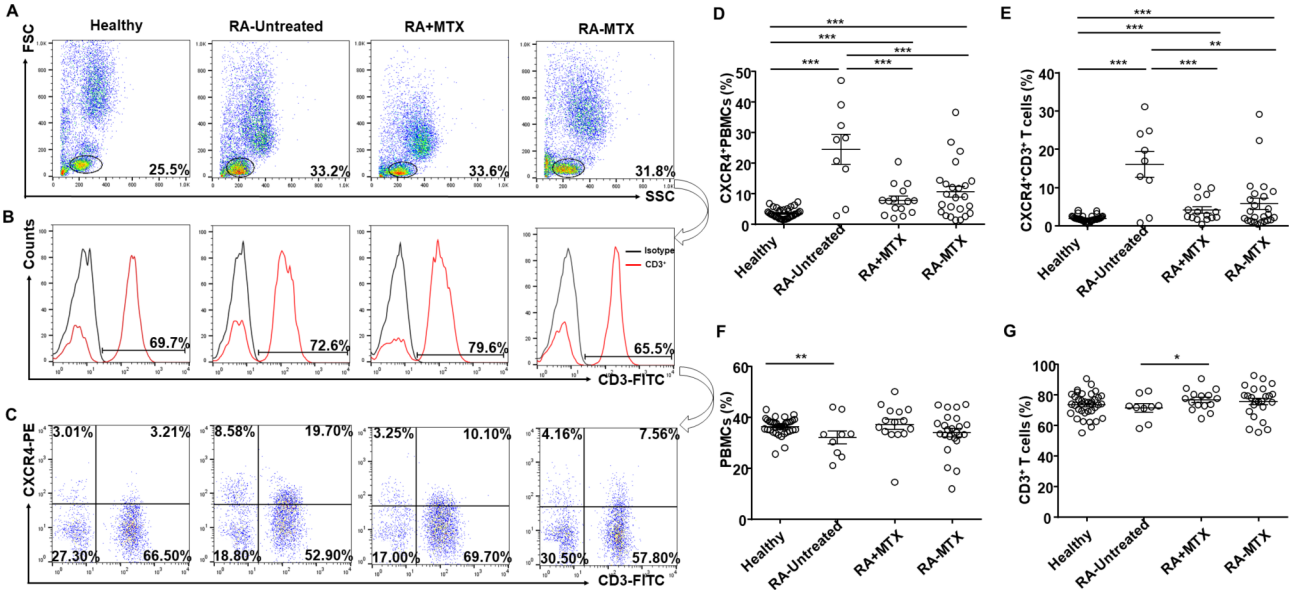

Fig. 1 Low dose MTX-treatment was clinically downregulated the frequency of CXCR4$^+$ immune cells in RA patients. (**A**-**C**) Representative flow charts demonstrating CXCR4$^+$ and CD3$^+$ T cells from both RA patients and healthy control. (**A**) Gating of human PBMCs. (**B**) CD3$^+$ T cells (stained with anti-human CD3 antibody, red) and Isotype controls (black). (**C**) Double staining with both anti-human CXCR4 and anti-human CD3 antibodies. Quantification of CXCR4$^+$PBMCs (**D**) and CXCR4$^+$CD3$^+$ T cells (**E**) from **A**-**C**. $^{**}p<0.01$, $^{***}p<0.001$ and error bars indicate SEM. Quantification of PBMCs (**F**) and CD3$^+$ T cells (**G**) from A-C. Healthy, (Normal control group, $n=37$); RA-Untreated (RA patients without clinical treatments, $n=9$); RA + MTX (RA patients treated with low dose MTX, $n=15$); RA-MTX (RA patients treated without low dose MTX, $n=24$)

S4A), CXCR4$^+$CD3$^+$ cells (Fig. S4B) were decreased in these groups, with an exception for the other group due to it including only three samples. PBMCs (Fig. S4C) and CD3$^+$ T cells (Fig. S4D) overall did not significantly change between RA-Untreated and the various RA-MTX clinic treatment groups. Patient's therapeutic outcomes were further evaluated according to the clinical diagnostic index (Fig. S5A-G). We found that patients' clinic scores of DAS28/ESR, DAS28/CRP, SDAI, TJC in 28 joints, PtGA, and PhGA showed significantly decrease after treatment with MTX and non-MTX drugs. Thus, these findings indicated that downregulation of CXCR4's expression in RA patients was associated with clinical treatments, including MTX.

Low dose MTX downregulates CXCR4's expression on lymphocytes

The use of low dose MTX has served as one of the most efficient drug treatments for RA patients in the clinic. Decreased CXCR4's expression in patients following MTX treatment indicated that low dose MTX could downregulate the expression of CXCR4. We tested the effects of 0.001–1 μg/mL MTX on the cell survival of human PBMCs. As shown in Fig. S6A-D, we found that 0.001 and 0.01 μg/mL MTX concentrations did not inhibit PBMCs survival in vitro, while the MTX doses between 0.1 and 1 μg/mL showed toxic effects on human PBMCs within 48 h. Hence, we chose 0.01 μg/mL MTX treat cells in the following experiments.

PBMCs and CD3$^+$ T cells from healthy subjects were optionally stimulated with anti-CD3 and anti-CD28 antibodies for 48 h in the absence or presence of 0.01 μg/mL MTX in vitro. In the non-stimulated cells, CXCR4$^+$PBMCs and CXCR4$^+$CD3$^+$ T cells were significantly decreased by 35.82±2.65% ($P<0.05$) and 40.48±5.65% ($P<0.05$) respectively after treatment with 0.01 g/mL MTX (Fig. 2A). Treatment with 0.01 μg/mL MTX in vitro did not result in significant changes of PBMCs and CD3$^+$ T cell numbers between vehicle and treatment groups (Fig. 2B). The qRT-PCR consistently showed that 0.01 μg/mL MTX-treatments decreased CXCR4 mRNA levels in both PBMCs and CD3$^+$ T cells by 70.75±1.30% ($P<0.001$) and 71.68±3.33% ($P<0.01$) (Fig. 2C). We also noticed that CXCR4 mRNA levels decreased by 54.40±5.66% ($P<0.01$) in 0.01 μg/mL MTX treated Jurkat cells (Fig. 2D), and increased DNA methylation in the -186 to -19 bp region of CXCR4 promoters in Jurkat cell after 0.01 μg/mL MTX treatment (Fig. 2E) for 48 h. Similarly, in the stimulated cells, CXCR4$^+$PBMCs and CXCR4$^+$CD3$^+$ T cells were significantly decreased by 23.32±1.80% ($P<0.05$) and 28.44±3.47% ($P<0.05$), (Fig. 2F), and the PBMCs and CD3$^+$ T cells numbers showed no significant changes respectively after treatment with 0.01 μg/mL MTX (Fig. 2G) for 48 h. We also detected CXCR4$^+$CD4$^+$ T cells and CXCR4$^+$CD8$^+$ T cells treated with 0.01 μg/mL MTX under activation states. The results showed that CXCR4$^+$CD4$^+$ T cells (Fig. S7B) and CXCR4$^+$CD8$^+$ T cells (Fig. S7D) were significantly

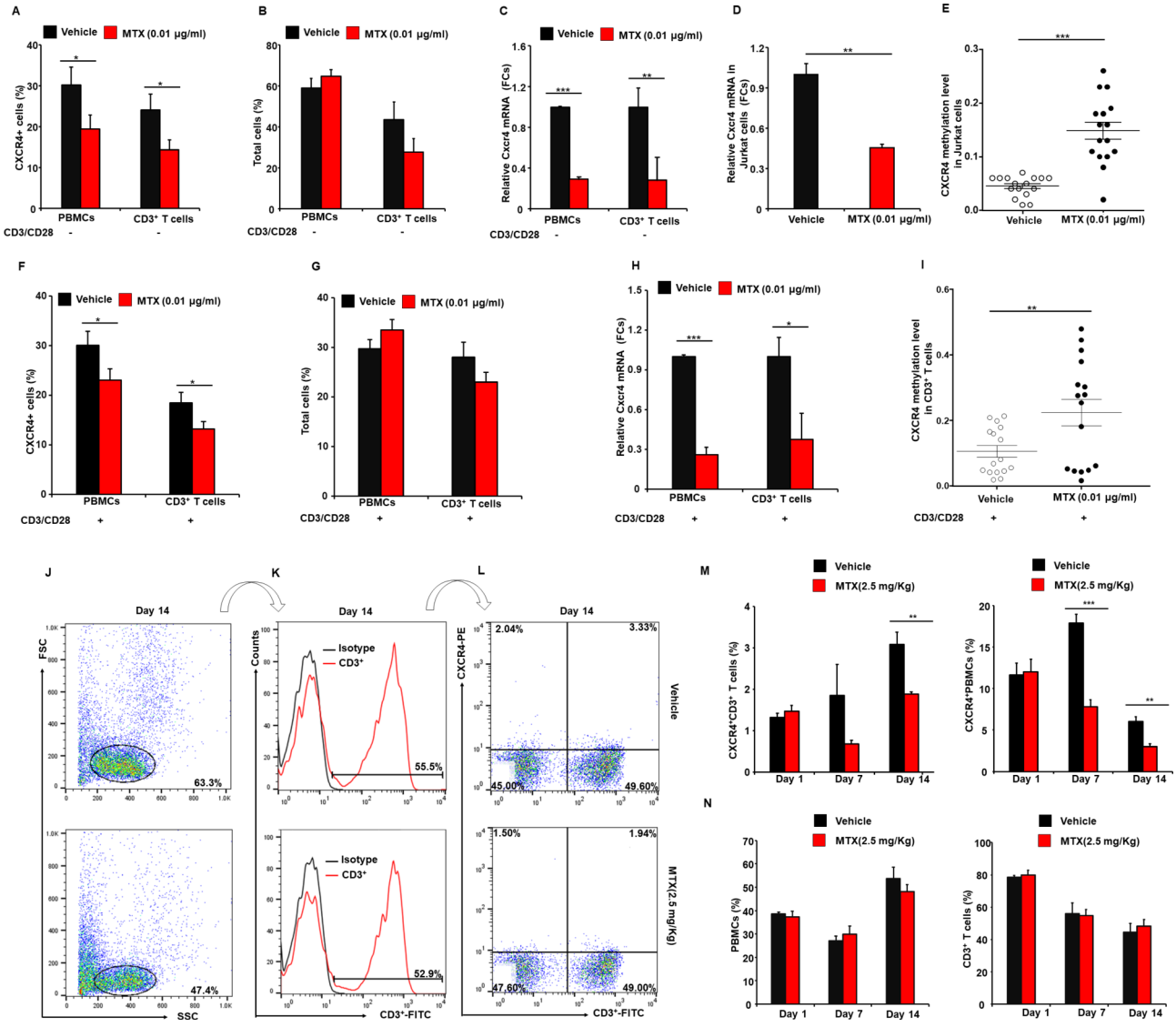

Fig. 2 Low dose MTX downregulated CXCR4's expression in normal human peripheral immune cells and mouse. (**A**-**C**) PBMCs from normal humans were non-stimulated with anti-CD3 and anti-CD28 for 48 h in the absence or presence of 0.01 μg/mL low dose MTX in vitro. (**A**) Quantification of human $CXCR4^+$PBMCs and $CXCR4^+CD3^+$ T cells (non-stimulated). (**B**) Quantification of human PBMCs and $CD3^+$ T cells (non-stimulated). (**C**-**D**) The qRT-PCR showing CXCR4's mRNA levels in human PBMCs and $CD3^+$ T cells (non-stimulated), Jurkat cells. (**E**) DNA methylation levels of CXCR4 promoter (-186 to -19 bp) in Jurkat cells after treatment with 0.01 μg/mL low dose MTX in vitro. (**F**-**I**) PBMCs from normal humans were stimulated with anti-CD3 and anti-CD28 for 48 h in the absence or presence of 0.01 μg/mL low dose MTX in vitro. (**F**-**G**) Quantification of human $CXCR4^+$/PBMCs and $CXCR4^+/CD3^+$, PBMCs and $CD3^+$ T cells (stimulated). (**H**) CXCR4's mRNA levels in human PBMCs and $CD3^+$ T cells (stimulated). (**I**) DNA methylation levels of CXCR4 promoter (-186 to -19 bp) in $CD3^+$ T cells (stimulated). Values on graphs represent mean ± SEM, $^*p<0.05$, $^{**}p<0.01$, $^{***}p<0.001$. (**J**-**L**) Representative flow charts showing $CXCR4^+CD3^+$ T cells after treatment with 2.5 mg/Kg MTX in vivo (see the details in Fig. S8). (**J**) Gating of mouse PBMCs. (**K**) Mouse $CD3^+$ T cells (stained with anti-mouse CD3 antibody, red, and Isotype controls, black). (**L**) Double staining with both anti-mouse CXCR4 and anti-mouse CD3 antibodies. (**M**) Quantification of $CXCR4^+CD3^+$ mouse T cells (left) and CXCR4-expressing mouse PBMCs (right) from J-L. (**N**) Quantification of mouse PBMCs (left) and mouse $CD3^+$ T cells (right) from J-L. (**M**-**N**) Data represented as mean ± SEM ($n=3$ normal mice, $^{**}p<0.01$, $^{***}p<0.001$)

decreased ($P<0.05$), and the percentage of $CD4^+$ T cells (Fig. S7A) and $CD8^+$ T cells (Fig. S7C) showed no significant changes, suggesting that the decrease of $CXCR4^+CD3^+$ T cells may be partly due to the decrease of $CXCR4^+CD4^+$ T cells and $CXCR4^+CD8^+$ T cell treatment with 0.01 μg/mL MTX. Furthermore, CXCR4 mRNA levels decreased by 74.00±4.36% ($P<0.001$) and 62.46±5.45% ($P<0.01$), respectively (Fig. 2H) in PBMCs and $CD3^+$ T cells, and DNA methylation increased in the -186 to -19 bp region of CXCR4 promoters in the activated $CD3^+$ T cells treated with 0.01 μg/mL MTX. Taken together, these results suggest that the decrease in CXCR4 mRNA levels are partly due to increased

DNA methylation of its promoter after 0.01 μg/mL MTX treatment.

We further tested the effect of low dose MTX on CXCR4's expression on PBMCs in normal mice. To address this question, healthy C57BL/6J mice were treated with the low dose of 2.5 mg/Kg MTX via gastric infusion (GI) three times per week, for a total of two weeks (Fig. S8A). The general animal survival (Fig. S8B) and animal weights (Fig. S8C) did not show any direct impact by low dose MTX. However, we observed low dose MTX significantly decreased the proportion of $CXCR4^{+}$PBMCs by 56.39±1.27% ($P<0.001$) at day 7 and by 50.11±3.82% ($P<0.01$) at day 14 (Fig. 2M-right). In the same manner, we found that $CXCR4^{+}CD3^{+}$ T cells was decreased by 39.07±7.72% ($P<0.01$) at day 14 due to the administration of low dose MTX (Fig. 2L and M-left). Similarly, the numbers of PBMCs (Fig. 2J and N-left) and $CD3^{+}$ T cells (Fig. 2K and N-right) cells did not show any significant changes between the vehicle and low does MTX treated mice. Here, we have provided evidence from both in vitro and in vivo studies to support the direct downregulating the expression of CXCR4 in peripheral immune cells by low dose MTX treatment.

Low dose MTX inhibits the transmigration of lymphocytes by downregulating CXCR4 expression

Due to CXCR4 widely functionally regulates the cell transmigration, hence, downregulation of CXCR4 by MTX suggests that low dose MTX may functionally regulate the transmigration of peripheral lymphocytes. To address this question, 100 ng/mL CXCL12 was applied to induce in vitro transmigration of activated healthy human PBMCs, followed by treating with 0.001–1 μg/mL MTX (Fig. 3A). Compared to the PBS control, we found that 0.01–1 μg/mL MTX decreased PBMCs' transmigration by approximately 35.29±5.20% ($P<0.05$) to 22.27±3.30% ($P<0.05$), indicating that 0.01–1 μg/mL MTX could efficiently inhibit the in vitro transmigration of human PBMCs. To verify the specificity of CXCL12's induction, we further applied a CXCR4-specific inhibitor

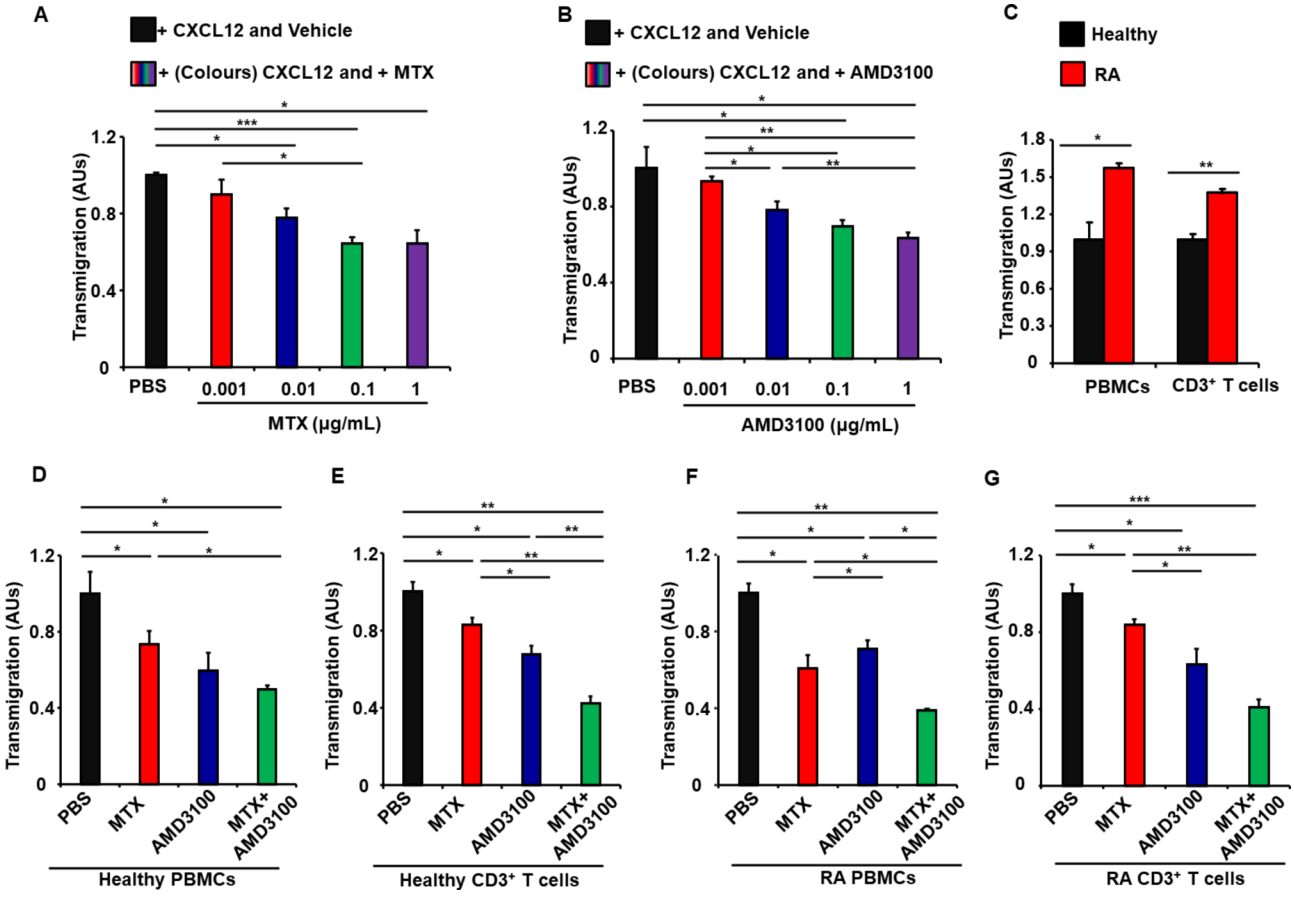

Fig. 3 Low dose MTX impaired CXCL12-induced $CD3^{+}$ T cell transmigration in vitro. (**A**-**B**) In vitro CXCL12-induced activated PBMC transmigration was blocked by MTX (**A**) and AMD3100 (**B**). (**A**-**B**) Added CXCL12 and Vehicle (100 ng/mL recombinant CXCL12-induced activated PBMCs treated with control vehicle), and added CXCL12 and MTX/AMD3100 (100 ng/mL recombinant CXCL12-induced activated PBMCs treated with 0.001 to 1 μg/mL MTX/AMD3100), and $n=3$ individual experiments. (**C**) PBMCs isolated from healthy and RA patients demonstrating different transmigration capacity ($n=3$ patients or healthy controls). (**D**-**G**) Combination of 0.01 μg/mL MTX and 1 μg/mL AMD3100 showing a synergistic inhibition for healthy controls and RA patients PBMCs and $CD3^{+}$ T cells, $n=3$ patients or healthy controls. (**A**-**G**) $^{*}P<0.05$, $^{**}P<0.01$, $^{***}p<0.001$. Data represented as mean ± SEM

AMD3100 to activated PBMCs' transmigration and observed dose-dependent inhibition of CXCL12-induced transmigration by AMD3100 (0.001–1 μg/mL) (Fig. 3B). These findings suggested that low dose MTX may regulate the transmigration of immune cells through downregulating the CXCR4's expression. Given that immune cells from RA patients expressed higher CXCR4, we further tested whether patients' immune cells contained more transmigration potency. Compared to the healthy control, we found that CXCL12-induced transmigration from both PBMCs and $CD3^+$ T cells were significantly increased by 57.40±9.88% ($P<0.05$) and 37.40±0.94% ($P<0.01$) respectively (Fig. 3C). More importantly, we observed a synergistic inhibitory effect with 0.01 μg/mL MTX and 1 μg/mL AMD3100 combined treatment on activated PBMCs and $CD3^+$ T cells isolated from healthy people (Fig. 3D-E) and RA patients (Fig. 3F-G). In summary, our results supported the inhibitory effect of low dose MTX-treatment on the transmigration of peripheral lymphocytes through downregulation of their CXCR4 expression.

MTX-mediated downregulation of CXCR4 to the treatment of AA mouse

Our studies suggested that downregulation of CXCR4 caused by low dose MTX may contribute to the effective clinical treatment of RA patients. To address this question, an AA mouse model was used to test the treatment effects from low dose MTX and AMD3100 (Fig. 4A). Consistent with previous studies [43], the AA mice developed typical severity scores of arthritic limbs (Fig. 4C). C57BL/6J wild type mice were preventatively administrated the doses of either 2.5 mg/Kg MTX or 5 mg/Kg AMD3100 per time for two weeks total treatment (5 times) (Fig. 4A). At day 15, mice were immunized with 150 μl CFA containing 4 mg/mL heat-killed *Mycobacterium tuberculosis*. Intradermal injection was conducted at three sites near the base of the tail according to the protocol from Brand et al. [40]. AA model mice were treated with low dose MTX or AMD3100 and 100% survival was observed at day 48 and the body weight were not affected between the four group mice (Fig. 4B, D).

At the pathological "peak" stage (day 25 to day 37), we observed that severity scores of arthritic limbs were significantly decreased after treatment with low dose MTX (Fig. 4C). For example, compared to untreated mice, clinical scores on day 31 had decreased by a maximum 8.7-fold change ($P<0.001$) after treatment with low dose MTX. However, no obvious clinical differences were observed from the pathological stages of "onset" (day 17–25). The effects of low dose MTX on $CXCR4^+$PBMCs were further examined at day 20 ("onset" stage), day 27 ("peak" stage), and day 38 ("recovery", day 38–48, stage). $CXCR4^+$PBMCs at day 20 was decreased by 33.50±5.88% ($P<0.05$) after treatment with low dose MTX compared with untreated AA mice (Fig. 4E). Because their total cells numbers were not changed (Fig. 4F), these observations suggested early preventatively effects from low dose MTX during the treatments. Conversely, we found that enhanced CXCR4's expression in untreated AA mice mainly appeared at later timepoints of day 27 compared with the Sham's (Sham versus AA Untreated). From the above observations, our results suggested that low dose MTX-mediated treatments may possibly rely on the suppression of CXCR4's function.

Furthermore, we observed that AMD3100 can efficiently treat AA mice (Fig. 4C). Compared with untreated AA mice, clinical scores at day 31 were decreased by a maximum 3.84-fold change ($P<0.001$) after treatment with AMD3100. The effect of AMD3100 was most significantly detected between day 25 to day 37 as well (AA Untreated versus AA+AMD3100). However, AMD3100 did not directly affect CXCR4's expression, but resulted in an abnormal accumulation of peripheral CXCR4-expressing cells. For instance, compared with untreated arthritis model mice, we noticed that the number of CXCR4-expressing cells increased by a 2.31-fold change ($P<0.01$) after AMD3100 treatments at day 20 (Fig. 4E, AA Untreated versus AA+AMD3100). Our findings suggest that both low dose MTX and CXCR4-specific inhibitor AMD3100 may share a similar mechanism to suppress immune cell migration during the treatment of arthritis mice.

Conditional knockout (CKO) of CXCR4 in peripheral immune cells in mouse

To explore the potential roles of CXCR4 in the arthritis mice model, we generated CXCR4 CKO ($CXCR4^{-/-}$) mice in which floxed *Cxcr4* gene was disrupted through the inducible *Cre* in peripheral blood cells. To accomplish this goal, Mx1-Cre transgenic mice ($Mx1\text{-}Cre^+/CXCR4^{+/+}$) and $Mx1\text{-}Cre^-/CXCR4^{flox/flox}$ mice both have a C57BL/6J background were founders to be crossbred to obtain $Mx1\text{-}Cre^+/CXCR4^{flox/flox}$ female mice (Fig. 5A). Between exon1 and exon2 of the *Cxcr4* gene, genotype primers were designed to amplify a 481-bp DNA for wild type (WT) *Cxcr4* allele and a 577-bp DNA floxed *Cxcr4* allele. In addition, primers to amplify a 408-bp DNA of *Cre* were designed to detect exogenous *Cre* gene. We detected a 577-bp of floxed *Cxcr4* band and a 408-bp of *Cre* band in the same mouse, supporting the successful generation of $Mx1\text{-}Cre^+/CXCR4^{flox/flox}$ mice (Fig. 5B). To disrupt the *Cxcr4* gene, $Mx1\text{-}Cre^+/CXCR4^{flox/flox}$ female mice were administrated with 12.5 mg/Kg PI: PC to induce Cre's expression through its inducible Mx1 promoter and generated a 569-bp *Cxcr4* genome DNA fragment (Fig. 5B-D). In addition, mice with different genotypes of either WT ($Mx1\text{-}cre^-/CXCR4^{+/+}$),

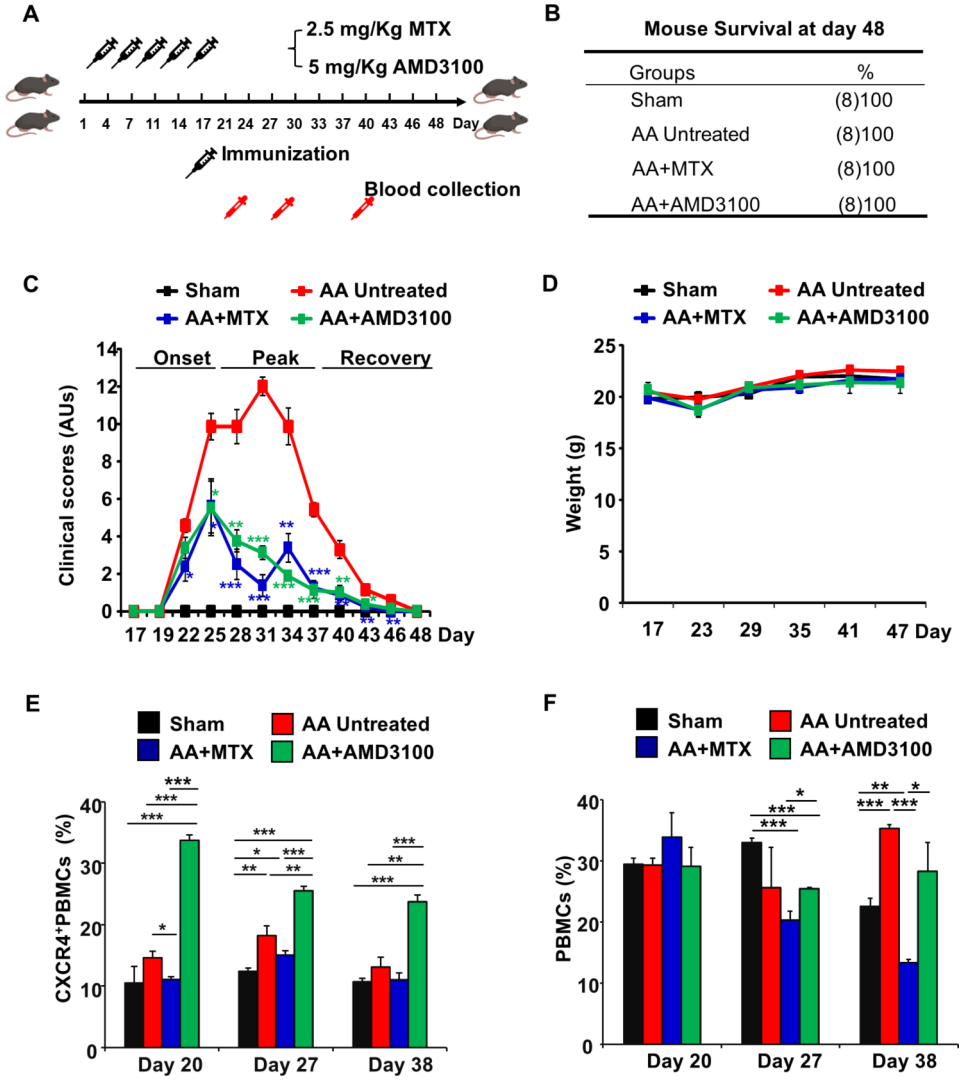

Fig. 4 Downregulation of the frequency of CXCR4$^+$ peripheral immune cells were associated with low dose MTX-mediated treatments in AA mice model. (**A**) Experimental design where wild type (WT) mice were pre-treated with 2.5 mg/Kg MTX or 5 mg/Kg AMD3100 before immunization. (**B**-**D**) Clinical characteristics of AA-related mice from A. (**B**) Survival, (**C**) Arthritic clinical scores and severity, (**D**) Weight. (**E**-**F**) Flow cytometry analysis of CXCR4-expressing mouse PBMCs ($n=3$ mice). CXCR4$^+$PBMCs (**E**) and PBMCs (**F**). (**C**-**F**) Sham (Mice without immunization), AA Untreated (Mice with immunization), AA + MTX (Mice with immunization after pretreating with 2.5 mg/Kg MTX), AA + AMD3100 (Mice with immunization after pretreating with 5 mg/Kg AMD3100). $^*P<0.05$, $^{**}P<0.01$, $^{***}P<0.001$, and data represented as mean ± SEM

Mx1-Cre$^+$ (Mx1-cre$^+$/CXCR4$^{+/+}$), or CXCR4$^{flox/flox}$ (Mx1-Cre$^-$/CXCR4$^{flox/flox}$) were injected by 12.5 mg/Kg PI: PC, and PI: PC did not affect their survival (Fig. 5E).

To verify the effects of PI: PC-induced CXCR4 CKO, peripheral PBMCs were isolated from the above mice and qRT-PCR was used to detect the mRNA levels of CXCR4 from their cells. Compared to WT, Mx1-Cre$^+$, or CXCR4$^{flox/flox}$ mice, expression of CXCR4's mRNA in Mx1-Cre$^+$/CXCR4$^{flox/flox}$ mice was decreased by 66.94±7.46% ($P<0.05$), 33.26±3.03% ($P<0.05$), and 72.32±1.59% ($P<0.05$) respectively (Fig. 5F). To confirm these observations, we further detected the CXCR4$^+$PBMCs by flow cytometry (Fig. 5G-H). Consistently, our results showed that CXCR4$^+$PBMCs from Mx1-Cre$^+$/CXCR4$^{flox/flox}$ mice was decreased by 61.38±0.96% ($P<0.01$), 71.19±3.41% ($P<0.001$), and 68.46±3.95% ($P<0.01$) when compared respectively with counterparts from WT, Mx1-Cre$^+$, or CXCR4$^{flox/flox}$ mice (Fig. 5H). More importantly, we found that transmigration of PBMCs from Mx1-Cre$^+$/CXCR4$^{flox/flox}$ mice was decreased by 48.58±3.08% ($P<0.001$), 33.94±4.60% ($P<0.01$), and 36.99±3.97% ($P<0.01$) when compared respectively with counterparts from WT, Mx1-Cre$^+$, or CXCR4$^{flox/flox}$ mice (Fig. 5I). Taken together with genotyping results, these findings supported a successful CXCR4 CKO mouse line by which the *Cxcr4* gene could be disrupted in peripheral PBMCs.

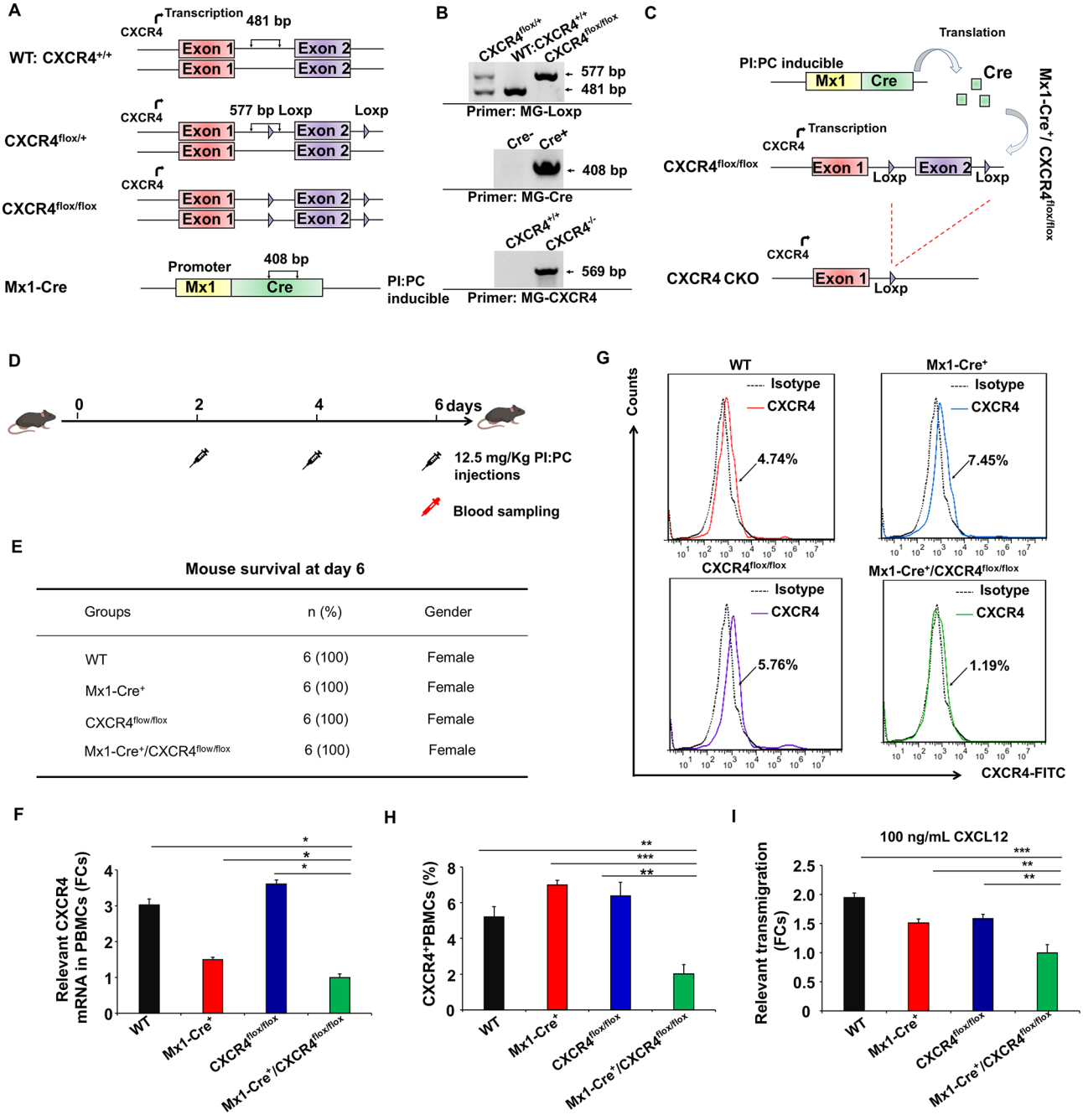

Fig. 5 Conditional deletion of *Cxcr4* in mouse's PBMCs. (**A**) Breeding and PCR-based genotyping designs for CXCR4 CKO mice. Mx1-Cre^{+} transgenic mice (Mx1-Cre^{+}/CXCR4$^{+/+}$) and Mx1-Cre^{-}/CXCR4$^{flox/flox}$ mice both have a C57BL/6J background were founders to be crossbred to obtain Mx1-Cre^{+}/CXCR4$^{flox/flox}$ mice. (**B**) Genomic PCR of mice tail biopsies. (**C**-**E**) Mx1-Cre^{+}/CXCR4$^{flox/flox}$ mice were administrated 12.5 mg/Kg PI: PC to induce Cre activity to specifically delete *Cxcr4* gene in PBMCs (See the details in Materials and methods). (**C**) Experimental design. (**D**) 12.5 mg/Kg PI: PC injection, and (**E**) Animal survival (all females, $n = 6$ mice). (**F**) The qRT-PCR analysis of *Cxcr4's* mRNA level in PBMCs from CXCR4 CKO mice. (**G**-**H**) Flow cytometry analysis of CXCR4^{+}PBMC from CXCR4 CKO mice. (**G**) Representative flow charts and (H) Quantitative analysis from G. (**I**) *Cxcr4*-deleted PBMCs loss of transmigration induced by 100 ng/mL recombinant CXCL12 in vitro. (**A**-**I**) Mouse genotypes indicted by Wild type (WT, Mx1-Cre^{-}/CXCR4$^{+/+}$), Mx1-Cre^{+} (Mx1-Cre^{+}/CXCR4$^{+/+}$), CXCR4$^{flox/flox}$ (Mx1-Cre^{-}/CXCR4$^{flox/flox}$), and Mx1-Cre^{+}/CXCR4$^{flox/flox}$ (*Cxcr4*-CKO). (**F**-**I**) Data represented as mean ± SEM, $^{*}p < 0.05$, $^{**}p < 0.01$ and $^{***}p < 0.001$

Loss of CXCR4 function in PBMCs resulted in decreased joint and lung inflammation in CIA mice

Above results indicate that the CXCL12-CXCR4 chemotaxis may play important roles during the pathological development of arthritis model mice. To address this hypothesis, we further explored whether disrupting CXCR4 in PBMCs could affect the pathogenesis of CIA mice (Fig. 6A). We noticed that although the WT CIA

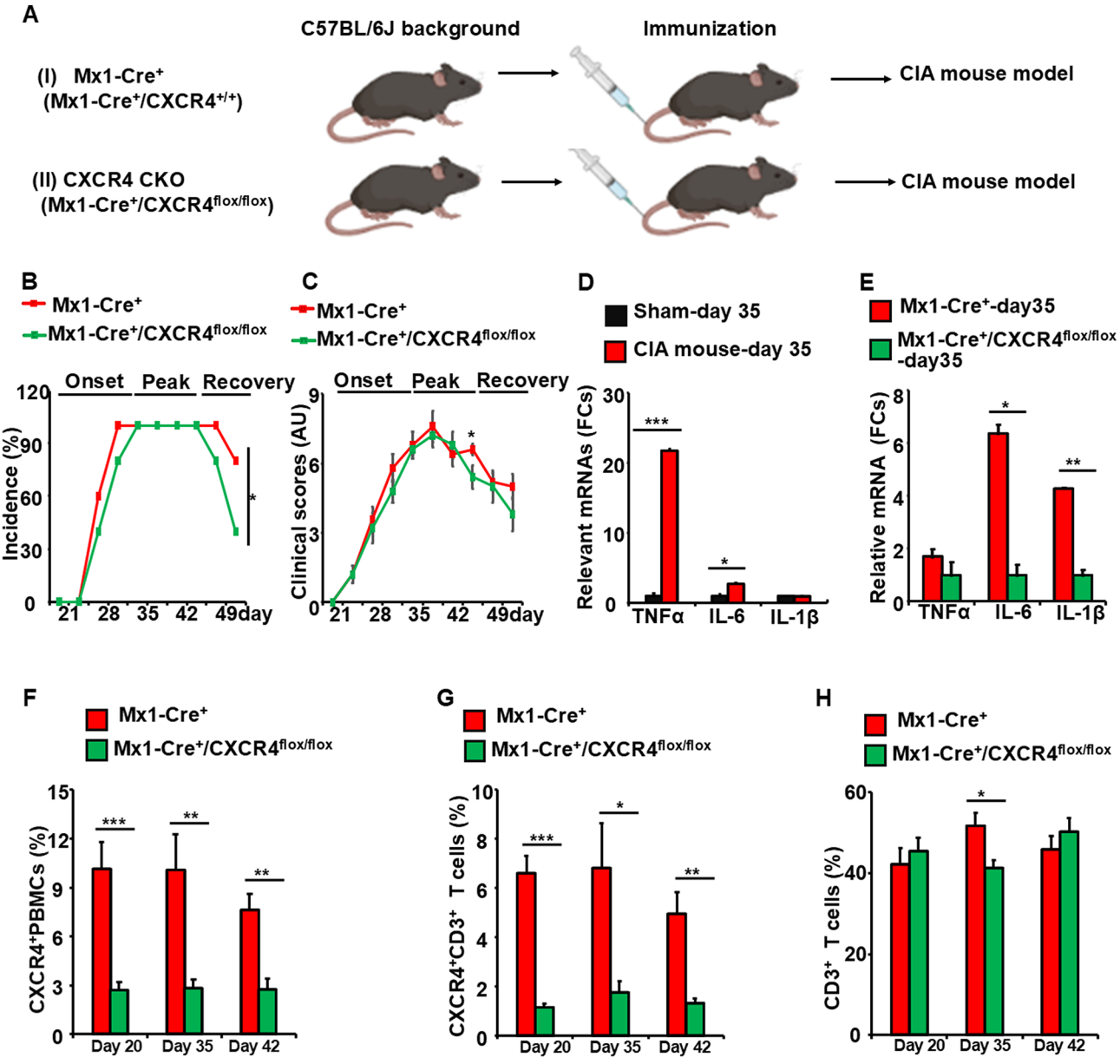

Fig. 6 Conditionally deleting *Cxcr4* gene in PBMCs decreased peripheral inflammation. (**A**) Experimental design of CIA mouse model using Mx1-Cre$^+$ (I, CXCR4-WT, Mx1-Cre$^+$/CXCR4$^{+/+}$) or CXCR4 CKO (II, Mx1-Cre$^+$/CXCR4$^{flox/flox}$) mice. (**B**) The incidence of arthritis. (**C**) The clinic scores of arthritis. (**D**) Enhanced lung inflammation observed in wild type CIA mice (Sham versus CIA mice). (**E**) The qRT-PCR analysis demonstrating decreased mRNA levels of inflammatory factors in the lung of CXCR4 CKO CIA mice compared with CXCR4-WT CIA mice at day 35. (**F**-**H**) Flow-based quantitative analysis demonstrating decreased the frequency of CXCR4$^+$ peripheral immune cells in CXCR4 CKO CIA mice. (**F**) CXCR4$^+$PBMCs. (**G**) CXCR4$^+$CD3$^+$ T cells. (**H**) Total CD3$^+$ T cells. (**D**) *$P < 0.05$ and ***$P < 0.001$, and $n = 4$ mice. (**E**-**H**) *$p < 0.05$, **$p < 0.01$ and ***$p < 0.001$, and $n = 5$ mice. Data represented as mean ± SEM

mice developed a three core arthritic stages (onset, peak and recovery stages) (Fig. S9A), loss of *Cxcr4* gene in peripheral blood cells did not directly impact this trend. However, the incidence of arthritis was decreased in Mx1-Cre$^+$/CXCR4$^{flox/flox}$ mice compared to Mx1-Cre$^+$ mice (Fig. 6B). The clinical scores of Mx1-Cre$^+$/CXCR4$^{flox/flox}$ mice were overall decreased compared with the Mx1-Cre$^+$ mice during the recover stage, and there was significantly decreased ($P<0.05$) at day 45 in Mx1-Cre$^+$/CXCR4$^{flox/flox}$ mice compared with Mx1-Cre$^+$ mice in CIA model mice (Fig. 6C). We further observed that cartilage destruction and bone erosion were significantly decreased (Fig. S10B-C), and local inflammation within the lungs were decreased after disrupting *Cxcr4* (**Fig. S10D-E**). To confirm this observation, inflammatory cytokines, such as TNFα, IL-6, and IL-1β from mice lung tissues, were further examined using qRT-PCR. In CIA mice, both TNFα's and IL-6's levels were increased by 21.81-fold change

($P<0.001$) and 2.72-fold change ($P<0.05$) when compared with Sham mice (Fig. 6D). We also found that IL-6's and IL-1β's mRNA levels from Mx1-Cre$^+$/CXCR4$^{flox/flox}$ CIA mice decreased significantly by a 6.36-fold change ($P<0.05$) and a 4.27-fold change ($P<0.01$) when compared with Mx1-Cre$^+$ CIA mice counterparts (Fig. 6E). Again, we noticed a decrease in CXCR4$^+$PBMCs and CXCR4$^+$CD3$^+$ T cells after disrupting the *Cxcr4* gene (Fig. 6F-H). These findings supported the potential effect of CXCR4 genetic disruption in eliminating both peripheral and local tissue inflammation in arthritis mice, suggesting a key role of the CXCL12-CXCR4 chemotaxis during the pathological development of RA diseases.

Discussion

Abnormal accumulation of immune cells within the synovial membrane [44], DNA hypomethylation [45, 46] are the major reason for the pathological development RA-related clinic scores. Under the inflammatory microenvironment, activated lymphocytes, dendritic cells and monocytes migrating from the peripheral blood cause the swollen synovial membrane, increased synovial fluid, and degraded cartilage in the joint. It has been suggested that migration of immune cells directly relies on multiple important chemotactic signals. For example, it has been reported that the expression of CXC chemokine CXCL12 is enhanced [47–49], both globally and in gene-specific hypomethylation of CXCL12 [50] in synovial cells in the joints of RA patients and is correlated with patient's pathological development [51, 52]. Recent studies have also suggested that both inflammatory cytokines and hypoxia could be the major factors that upregulated the expression of CXCL12 in patient's joints [53–55]. Other than the local tissue environment, it has been reported that the plasma level of the CXCL12 protein was increased in RA patients as well [30]. These findings potentially support the hypothesis that elevated CXCL12 within the synovium may provide the important chemoattractant for immune cell migration during the pathological development of RA diseases.

Meanwhile, CXCL12 and its cognate receptor CXCR4 mediate a key chemotaxis responsible for immune cell migration [8]. As such, it is possible that CXCR4-expressing immune cells from both peripheral blood and synovium may contribute to the pathogenesis of RA. Recent studies have observed that expression of CXCR4 is upregulated in dendritic cells and memory T cells in the synovium from RA patients when compared against healthy controls [9, 56, 57]. In the current study, we examined the frequency of CXCR4$^+$PBMCs and CXCR4$^+$CD3$^+$ T cells on RA patients. Compared to healthy group, RA patients exhibited a higher frequency of both CXCR4$^+$PBMCs and CXCR4$^+$CD3$^+$ T cells. Enhanced CXCR4$^+$ immune cells is potentially correlated with the inflammatory cytokines in patients' plasma. These observations further supported previous findings reporting elevated expression of CXCR4 in peripheral CD4$^+$ Th17$^+$ T cells in RA patients [56, 58]. Increased CXCR4$^+$ immune cells not only appeared in synovial fluid within the joint but also in the peripheral blood in RA patients. These findings indicate that enhanced CXCR4$^+$ immune cells in peripheral blood may represent some early events that potentially contribute to the pathological development of RA diseases.

In the current study, we also found that clinical treatments potentially downregulate the frequency of CXCR4$^+$ immune cells in RA patients. High-dose and low-dose MTX have been widely used to treat cancer or autoimmune diseases. However, the potential targets for this drug are still not well understood. A study indicating that global DNA hypomethylation can be reversed with MTX treatment in bulk T cells from patients with RA [35]. Recent studies suggested that CXCL12 was increased in blood in rats treated with high dose MTX. However, a high dose of MTX did change the CXCL12 levels in bone marrow from the same groups of rats [59]. Different from high dose MTX, Hansen et al. (2006) reported that low dose MTX did not change the blood levels of CXCL12 in RA patients [30]. These findings suggest the effect of MTX on CXCL12 truly depends on drug's concentrations and tissue types treated.

As for CXCR4, it has been reported that CXCR4's expression in rat's hematopoietic stem cells was decreased after treatment with high dose MTX [59]. High dose MTX upregulated the expression of CXCR4 in colon cancer cells [60]. Conversely, low dose MTX downregulated CXCR4's expression in treated synovium of rats [61]. In the current study, we observed that the downregulation of CXCR4$^+$PBMCs and CXCR4$^+$CD3$^+$ T cells was associated with the treatments of low dose MTX in RA patients. Our in vitro studies showed that low dose MTX reverted hypomethylation of promoter CpG sites in Jurkat and CD3$^+$ T cell, which lead to the downregulated mRNA expression of CXCR4. Consistently, low dose MTX inhibited the transmigration that was induced by CXCL12, a similar observation obtained from using CXCR4-specific inhibitor AMD3100. Our studies further showed that both low dose MTX and AMD3100 can treat RA-related diseases in the arthritis mouse model. The treatments using low dose MTX may rely on the functions of CXCR4, particularly in peripheral immune cells. However, the potential regulation of other chemokine receptors by low dose MTX cannot be fully excluded. These results suggest that low dose MTX decreased the migration capacity of immune cells through downregulation of CXCR4 expression due to the hypermethylation. However, these effects were not limited to low dose MTX, as other clinical treatments were also found to downregulate the frequency of CXCR4$^+$

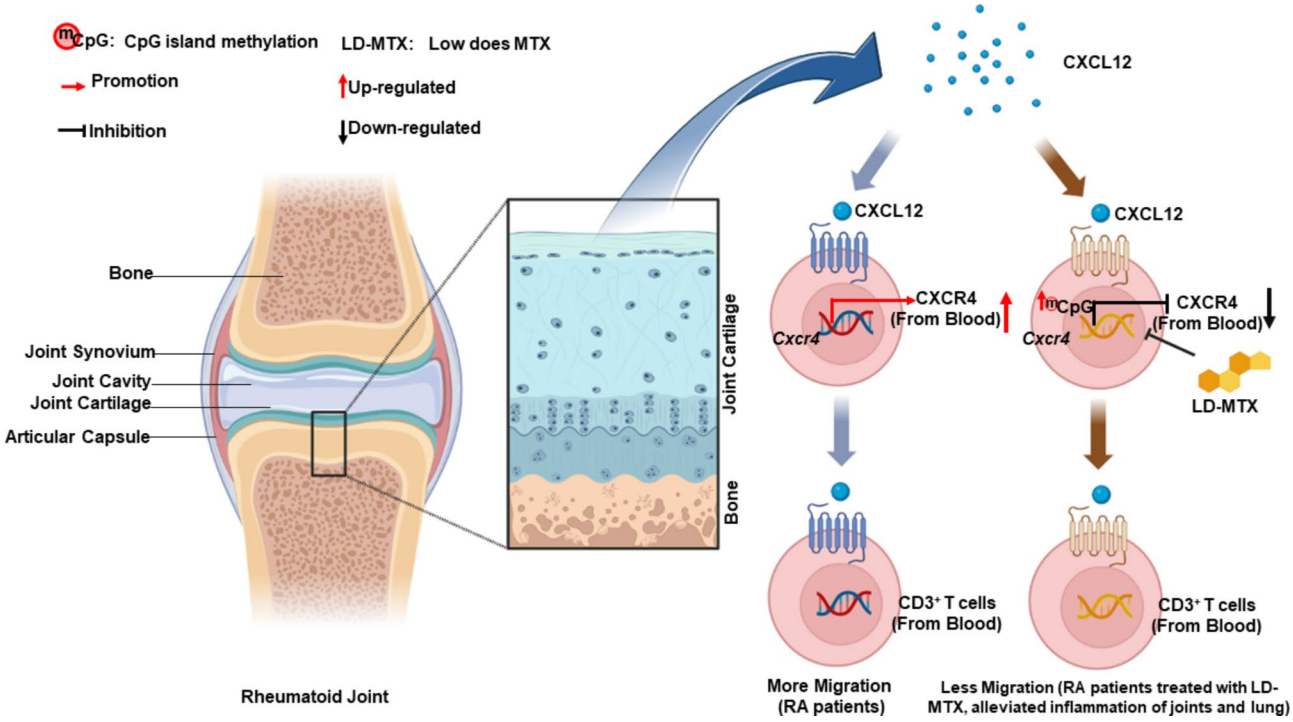

Fig. 7 The Proposed schematic model for low dose MTX impaired T cell transmigration through down-regulating CXCR4 expression in RA patients. The increased $CXCR4^+$PBMCs and $CXCR4^+CD3^+$ T cells in RA patients' peripheral immune cells caused more cell migration capacity to promote the development of RA. CXCR4's expression on peripheral immune cells was significantly downregulated after low dose MTX treatment due to the increased genomic hypermethylation across the promoter region of *Cxcr4* gene, mediating the decrease of cell transmigration in vitro, which significantly improved the pathological development of RA partly through potentially alleviated inflammation of joints and lung tissue in RA patients

peripheral immune cells in RA patients. The CXCL12-CXCR4 chemotaxis may represent the universal molecular pathway involved in both pathological development and treatment of RA patients. Therefore, the detailed mechanism underlying low dose MTX-mediated treatments in RA patients still remains relatively unknown and open for further future investigation.

Chung et al. (2010) reported that the incidence, but not the severity, of CIA was significantly reduced in T cell-specific *Cxcr4*-deficient mice [16]. Since expression of CXCR4 is not limited to T cells, we further explored the roles of CXCR4 in peripheral immune cells by generating mice with Mx1-Cre/$CXCR4^{flox/flox}$ genotype. A broader genetic disruption of *Cxcr4* gene in different peripheral immune cells from Mx1-Cre/$CXCR4^{flox/flox}$ mice was induced by PI: PC. We also noticed a little improvement in CXCR4 CKO mice compared with *Cxcr4* WT mice during the recovery phase. In addition, we observed that both peripheral and lungs' inflammations were significantly eliminated in CXCR4 CKO mice. Our loss of function studies supported the significance of CXCR4's role during the pathological development of RA. Even so, most human trials of anti-chemokine signaling pathways have failed to show clinical improvements [7], suggesting CXCL12-CXCR4 is not the only chemotaxis related to RA's pathogenesis. Therefore, to fully grasp the detailed mechanism associated with chemokine signaling underlying low dose MTX and other clinic treatments in RA patients, a more thorough investigation must be conducted in the future.

Conclusions

In summary, this study found that the frequency of $CXCR4^+$PBMCs and $CXCR4^+CD3^+$ T cells were increased in RA patients. Following, CXCR4's expression or the frequency of $CXCR4^+$PBMCs and $CXCR4^+CD3^+$ T cells on peripheral immune cells was significantly downregulated after treated with low dose MTX treatment in vitro and in vivo. Consistently, the capacity of immune cell transmigration was inhibited by down-regulated expression of chemokine receptor CXCR4. Briefly, in vitro, low dose MTX significantly decreased cell transmigration through down-regulated CXCR4's expression caused by an increased genomic hypermethylation across the promoter region of *Cxcr4* gene in $CD3^+$ T cells. In vivo, low dose MTX-mediated downregulate the frequency of $CXCR4^+$PBMCs and $CXCR4^+CD3^+$ T cells significantly improved the pathological development of mouse arthritis models. Moreover, the conditional disruption of the *Cxcr4* gene in peripheral immune cells potentially alleviated inflammation of joints and lung tissues in the arthritis mice (Fig. 7). Our results

taken together suggested that the effect of low dose MTX treatment could serve to eliminate inflammation in RA patients through impairment of immune cell transmigration due to the down-regulated expression of chemokine receptor CXCR4.

Abbreviations

cDNA	Complement DNA
CFA	Complete freund's adjuvant
CIA	Collagen-induced arthritis
CII	Type II collagen
CKO	Conditional knockout
CXCR4	CXC motif chemokine receptor 4
DHFR	Inhibiting dihydrofolate reductase
ECM	Extracellular matrix
ELISA	Enzyme-linked immunosorbent assay
FCM	Flow cytometry
GRO/CXCR1	Chemokine (CXC motif) ligand 1
H&E	Hematoxylin and eosin
IL-1β	Interleukin 1 beta
IL-1r	Interleukin 1 receptor type 1
IL-6	Interleukin 6
IL-8	Interleukin 8
IL-17R	Interleukin 17 receptor A
MCP-1/CCL2	C-C motif chemokine ligand 2
MTX	Methotrexate
NS	Normal saline
PBMC	Peripheral blood mononuclear cells
PFA	Paraformaldehyde
PI	PC: Polyinosinic-polycytidylic acid
PMT	Photomultiplier tube
qRT-PCR	Quantitative real-time polymerase chain reaction
RA	Rheumatoid arthritis
RANTES /CCL5	C-C motif chemokine ligand 5
SDF-1/CXCL12	CXC motif chemokine ligand 12
SEM	Standard error of mean
TNF-α	Tumor necrosis factor alpha
TGFB1	TGF-beta 1

Supplementary Information

The online version contains supplementary material available at https://doi.org/10.1186/s13075-024-03403-9.

Supplementary Material 1

Acknowledgements

We thank professor Shenghong Li (Institute of Botany, the Chinese Academy of Sciences, Kunming, China) kindly providing Jurkat cells. We thank Dr. Wei Wang and Dr. Guiyuan Chen for their assistance to collect patient sample collection, isolate PBMCs, establish arthritis mice model and conduct flow cytometry experiments. We thank Dr. Wei Wang who worked in the Department of Rheumatology from First Affiliated Hospital of Kunming Medical University and studied in the School of Life Sciences of Yunnan University for kindly providing human blood specimens and clinical RA diagnosis.

Author contributions

Conception and design (Lei Ding, Daniel H. Park, Bo Gao, Meizhang Li, Haitham Abedelhakim, and Ming Zhang). Experiments and data analysis (Lei Ding, Daniel H. Park, Bo Gao, Meizhang Li, Haitham Abedelhakim, and Ming Zhang). Manuscript preparation (Lei Ding, Daniel H. Park, Meizhang Li, Haitham Abedelhakim, and Ming Zhang). Reviewed and edited the manuscript (Lei Ding, Daniel H. Park, Bo Gao, Lingyuan Wu, Meizhang Li, Haitham Abedelhakim, and Ming Zhang). All authors of this paper have read and approved the final version submitted.

Funding

This work was financially supported by the Talent Program of Yunnan Province (No. 2011HA009), the Youth Project of the Science and Technology Department of Yunnan Province (No. 202001BB050041), and the National Natural Science Foundation of China (No. 32360165, 31660273).

Data availability

Data and full uncropped Gels are provided within the related information files.

Declarations

Ethics approval and consent to participate

The study was performed in accordance with the ethical standards of the institutional and national research committee and with the 1964 Helsinki Declaration and its later amendments. This study was approved by both the Ethics Committee of the First Affiliated Hospital of Kunming Medical University and the Committee on Human Subject Research and Ethics of Yunnan University (Approved number: 20190801). All experiments were carried out according to the relevant guidelines. All animal studies and relevant procedures were reviewed and approved by the ethics committee of the institutional animal care and use committee, Yunnan University (IACUC, YNU) (Approved number: 20190801). Written informed consent for the present study's use of human peripheral blood was obtained from all forty-eight patients and thirty-seven healthy donors (HDs).

Consent for publication

Written informed consent for the publication was obtained from the study participants.

Competing interests

The authors declare no competing interests.

Received: 22 November 2023 / Accepted: 17 September 2024
Published online: 30 September 2024

References

1. McInnes IB, Schett G. The pathogenesis of rheumatoid arthritis. N Engl J Med. 2011;365(23):2205–19.
2. Buckley CD. Science, medicine, and the future. Treatment of rheumatoid arthritis. BMJ. 1997;315(7102):236–8.
3. Salmon M, Gaston JS. The role of T-lymphocytes in rheumatoid arthritis. Br Med Bull. 1995;51(2):332–45.
4. Elemam NM, Hannawi S, Maghazachi AA. Role of chemokines and Chemokine receptors in Rheumatoid Arthritis. Immunotargets Ther. 2020;9:43–56.
5. Vergunst CE, van de Sande MG, Lebre MC, Tak PP. The role of chemokines in rheumatoid arthritis and osteoarthritis. Scand J Rheumatol. 2005;34(6):415–25.
6. Szekanecz Z, Kim J, Koch AE. Chemokines and chemokine receptors in rheumatoid arthritis. Semin Immunol. 2003;15(1):15–21.
7. Szekanecz Z, Koch AE. Successes and failures of chemokine-pathway targeting in rheumatoid arthritis. Nat Rev Rheumatol. 2016;12(1):5–13.
8. Li M, Ransohoff RM. Multiple roles of chemokine CXCL12 in the central nervous system: a migration from immunology to neurobiology. Prog Neurobiol. 2008;84(2):116–31.
9. Nanki T, Hayashida K, El-Gabalawy HS, Suson S, Shi K, Girschick HJ, Yavuz S, Lipsky PE. Stromal cell-derived factor-1-CXC chemokine receptor 4 interactions play a central role in CD4 + T cell accumulation in rheumatoid arthritis synovium. J Immunol. 2000;165(11):6590–8.
10. Bradfield PF, Amft N, Vernon-Wilson E, Exley AE, Parsonage G, Rainger GE, et al. Rheumatoid fibroblast-like synoviocytes overexpress the chemokine stromal cell-derived factor 1 (CXCL12), which supports distinct patterns and rates of CD4 + and CD8 + T cell migration within synovial tissue. Arthritis Rheum. 2003;48(9):2472–82.
11. Buckley CD, Amft N, Bradfield PF, Pilling D, Ross E, Arenzana-Seisdedos F, et al. Persistent induction of the chemokine receptor CXCR4 by TGF-beta 1 on synovial T cells contributes to their accumulation within the rheumatoid synovium. J Immunol. 2000;165(6):3423–9.

12. Shadidi KR, Aarvak T, Henriksen JE, Natvig JB, Thompson KM. The chemokines CCL5, CCL2 and CXCL12 play significant roles in the migration of Th1 cells into rheumatoid synovial tissue. Scand J Immunol. 2003;57(2):192–8.
13. Lenoir M, Djerdjouri B, Perianin A. Stroma cell-derived factor 1alpha mediates desensitization of human neutrophil respiratory burst in synovial fluid from rheumatoid arthritic patients. J Immunol. 2004;172(11):7136–43.
14. Matthys P, Hatse S, Vermeire K, Wuyts A, Bridger G, Henson GW, De Clercq E, Billiau A, Schols D. AMD3100, a potent and specific antagonist of the stromal cell-derived factor-1 chemokine receptor CXCR4, inhibits autoimmune joint inflammation in IFN-gamma receptor-deficient mice. J Immunol. 2001;167(8):4686–92.
15. De Klerck B, Geboes L, Hatse S, Kelchtermans H, Meyvis Y, Vermeire K, et al. Pro-inflammatory properties of stromal cell-derived factor-1 (CXCL12) in collagen-induced arthritis. Arthritis Res Ther. 2005;7(6):R1208–20.
16. Chung SH, Seki K, Choi BI, Kimura KB, Ito A, Fujikado N, Saijo S, Iwakura Y. CXC chemokine receptor 4 expressed in T cells plays an important role in the development of collagen-induced arthritis. Arthritis Res Ther. 2010;12(5):R188.
17. Bedoui Y, Guillot X, Selambarom J, Guiraud P, Giry C, Jaffar-Bandjee MC, Ralandison S, Gasque P. Methotrexate an Old Drug with New tricks. Int J Mol Sci 2019; 20(20).
18. Visentin M, Zhao R, Goldman ID. The antifolates. Hematol Oncol Clin North Am. 2012;26(3):629–48. ix.
19. Weinblatt ME, Maier AL, Coblyn JS. Low dose leucovorin does not interfere with the efficacy of methotrexate in rheumatoid arthritis: an 8 week randomized placebo controlled trial. J Rheumatol. 1993;20(6):950–2.
20. Whittle SL, Hughes RA. Folate supplementation and methotrexate treatment in rheumatoid arthritis: a review. Rheumatology (Oxford). 2004;43(3):267–71.
21. Friedman B, Cronstein B. Methotrexate mechanism in treatment of rheumatoid arthritis. Joint Bone Spine. 2019;86(3):301–07.
22. Cronstein BN, Aune TM. Methotrexate and its mechanisms of action in inflammatory arthritis. Nat Rev Rheumatol. 2020;16(3):145–54.
23. Deleuran B, Kristensen M, Paludan K, Zachariae C, Larsen CG, Zachariae E, Thestrup-Pedersen K. The effect of second-line antirheumatic drugs on interleukin-8 mRNA synthesis and protein secretion in human endothelial cells. Cytokine. 1992;4(5):403–9.
24. Boiardi L, Macchioni P, Meliconi R, Pulsatelli L, Facchini A, Salvarani C. Relationship between serum RANTES levels and radiological progression in rheumatoid arthritis patients treated with methotrexate. Clin Exp Rheumatol. 1999;17(4):419–25.
25. Yoshida M, Kanno Y, Ishisaki A, Tokuda H, Hirade K, Nakajima K, Katagiri Y, Shimizu K, Kozawa O. Methotrexate suppresses inflammatory agonist induced interleukin 6 synthesis in osteoblasts. J Rheumatol. 2005;32(5):787–95.
26. Gao lK, Leins C, Bohlen H, Heilig B, Lemmel EM. Inhibition of interleukin-8 synthesis by intraarticular methotrexate therapy in patients with rheumatoid arthritis. Z Rheumatol. 1998;57(2):95–100.
27. Seitz M, Loetscher P, Dewald B, Towbin H, Rordorf C, Gallati H, Gerber NJ. Interleukin 1 (IL-1) receptor antagonist, soluble tumor necrosis factor receptors, IL-1 beta, and IL-8–markers of remission in rheumatoid arthritis during treatment with methotrexate. J Rheumatol. 1996;23(9):1512–6.
28. Seitz M, Dewald B, Ceska M, Gerber N, Baggiolini M. Interleukin-8 in inflammatory rheumatic diseases: synovial fluid levels, relation to rheumatoid factors, production by mononuclear cells, and effects of gold sodium thiomalate and methotrexate. Rheumatol Int. 1992;12(4):159–64.
29. Brandalise SR, Assis R, Laranjeira ABA, Yunes JA, de Campos-Lima PO. Low-dose methotrexate in sickle-cell disease: a pilot study with rationale borrowed from rheumatoid arthritis. Exp Hematol Oncol. 2017;6:18.
30. Hansen IB, Ellingsen T, Hornung N, Poulsen JH, Lottenburger T, Stengaard-Pedersen K. Plasma level of CXC-chemokine CXCL12 is increased in rheumatoid arthritis and is independent of disease activity and methotrexate treatment. J Rheumatol. 2006;33(9):1754–9.
31. Abdelaal NH, Elhefnawy NG, Abdulmonem SR, Sayed S, Saleh NA, Saleh MA. Evaluation of the expression of the stromal cell-derived factor-1 alpha (CXCL 12) in psoriatic patients after treatment with Methotrexate. J Cosmet Dermatol. 2020;19(1):253–58.
32. Barsig J, Yam G, Lehner MD, Beume R. Methotrexate treatment suppresses local cytokine and chemokine production in rat adjuvant arthritis. Drugs Exp Clin Res. 2005;31(1):7–11.
33. Kehlen A, Thiele K, Riemann D, Langner J. Expression, modulation and signalling of IL-17 receptor in fibroblast-like synoviocytes of patients with rheumatoid arthritis. Clin Exp Immunol. 2002;127(3):539–46.
34. Kim YI, Logan JW, Mason JB, Roubenoff R. DNA hypomethylation in inflammatory arthritis: reversal with methotrexate. J Lab Clin Med. 1996;128(2):165–72.
35. de Andres MC, Perez-Pampin E, Calaza M, Santaclara FJ, Ortea I, Gomez-Reino JJ, Gonzalez A. Assessment of global DNA methylation in peripheral blood cell subpopulations of early rheumatoid arthritis before and after methotrexate. Arthritis Res Ther. 2015;17(1):233.
36. Guderud K, Sunde LH, Flam ST, Maehlen MT, Mjaavatten MD, Norli ES, et al. Methotrexate Treatment of newly diagnosed RA patients is Associated with DNA methylation differences at Genes Relevant for Disease Pathogenesis and Pharmacological Action. Front Immunol. 2021;12:713611.
37. Arnett FC, Edworthy SM, Bloch DA, McShane DJ, Fries JF, Cooper NS, et al. The American Rheumatism Association 1987 revised criteria for the classification of rheumatoid arthritis. Arthritis Rheum. 1988;31(3):315–24.
38. Sun C, McAndrew T, Smith BC, Chen Z, Frimer M, Burk RD. Characterization of HPV DNA methylation of contiguous CpG sites by bisulfite treatment and massively parallel sequencing-the FRAGMENT approach. Front Genet. 2014;5:150.
39. Kollias G, Papadaki P, Apparailly F, Vervoordeldonk MJ, Holmdahl R, Baumans V, et al. Animal models for arthritis: innovative tools for prevention and treatment. Ann Rheum Dis. 2011;70(8):1357–62.
40. Brand DD, Latham KA, Rosloniec EF. Collagen-induced arthritis. Nat Protoc. 2007;2(5):1269–75.
41. Weinberger A, Halpern M, Zahalka MA, Quintana F, Traub L, Moroz C. Placental immunomodulator ferritin, a novel immunoregulator, suppresses experimental arthritis. Arthritis Rheum. 2003;48(3):846–53.
42. Gao B, Lin J, Jiang Z, Yang Z, Yu H, Ding L, et al. Upregulation of chemokine CXCL10 enhances chronic pulmonary inflammation in tree shrew collagen-induced arthritis. Sci Rep. 2018;8(1):9993.
43. Inglis JJ, Simelyte E, McCann FE, Criado G, Williams RO. Protocol for the induction of arthritis in C57BL/6 mice. Nat Protoc. 2008;3(4):612–8.
44. Leblond A, Allanore Y, Avouac J. Targeting synovial neoangiogenesis in rheumatoid arthritis. Autoimmun Rev. 2017;16(6):594–601.
45. Javierre BM, Hernando H, Ballestar E. Environmental triggers and epigenetic deregulation in autoimmune disease. Discov Med. 2011;12(67):535–45.
46. Meda F, Folci M, Baccarelli A, Selmi C. The epigenetics of autoimmunity. Cell Mol Immunol. 2011;8(3):226–36.
47. Kim HR, Kim KW, Kim BM, Jung HG, Cho ML, Lee SH. Reciprocal activation of CD4 + T cells and synovial fibroblasts by stromal cell-derived factor 1 promotes RANKL expression and osteoclastogenesis in rheumatoid arthritis. Arthritis Rheumatol. 2014;66(3):538–48.
48. Nanki T, Nagasaka K, Hayashida K, Saita Y, Miyasaka N. Chemokines regulate IL-6 and IL-8 production by fibroblast-like synoviocytes from patients with rheumatoid arthritis. J Immunol. 2001;167(9):5381–5.
49. Watanabe N, Ando K, Yoshida S, Inuzuka S, Kobayashi M, Matsui N, Okamoto T. Gene expression profile analysis of rheumatoid synovial fibroblast cultures revealing the overexpression of genes responsible for tumor-like growth of rheumatoid synovium. Biochem Biophys Res Commun. 2002;294(5):1121–9.
50. Karouzakis E, Rengel Y, Jungel A, Kolling C, Gay RE, Michel BA, et al. DNA methylation regulates the expression of CXCL12 in rheumatoid arthritis synovial fibroblasts. Genes Immun. 2011;12(8):643–52.
51. Kanbe K, Chiba J, Inoue Y, Taguchi M, Yabuki A. SDF-1 and CXCR4 in synovium are associated with disease activity and bone and joint destruction in patients with rheumatoid arthritis treated with golimumab. Mod Rheumatol. 2016;26(1):46–50.
52. Grassi F, Cristino S, Toneguzzi S, Piacentini A, Facchini A, Lisignoli G. CXCL12 chemokine up-regulates bone resorption and MMP-9 release by human osteoclasts: CXCL12 levels are increased in synovial and bone tissue of rheumatoid arthritis patients. J Cell Physiol. 2004;199(2):244–51.
53. Santiago B, Calonge E, Del Rey MJ, Gutierrez-Canas I, Izquierdo E, Usategui A, Galindo M, Alcami J, Pablos JL. CXCL12 gene expression is upregulated by hypoxia and growth arrest but not by inflammatory cytokines in rheumatoid synovial fibroblasts. Cytokine. 2011;53(2):184–90.
54. Iwamoto T, Okamoto H, Toyama Y, Momohara S. Molecular aspects of rheumatoid arthritis: chemokines in the joints of patients. FEBS J. 2008;275(18):4448–55.
55. Hitchon C, Wong K, Ma G, Reed J, Lyttle D, El-Gabalawy H. Hypoxia-induced production of stromal cell-derived factor 1 (CXCL12) and vascular endothelial growth factor by synovial fibroblasts. Arthritis Rheum. 2002;46(10):2587–97.
56. Lande R, Giacomini E, Serafini B, Rosicarelli B, Sebastiani GD, Minisola G, et al. Characterization and recruitment of plasmacytoid dendritic cells in synovial fluid and tissue of patients with chronic inflammatory arthritis. J Immunol. 2004;173(4):2815–24.
57. Perretti M, Ingegnoli F, Wheller SK, Blades MC, Solito E, Pitzalis C. Annexin 1 modulates monocyte-endothelial cell interaction in vitro and cell migration

in vivo in the human SCID mouse transplantation model. J Immunol. 2002;169(4):2085–92.
58. Burska AN, Thu A, Parmar R, Bzoma I, Samans B, Raschke E, et al. Quantifying circulating Th17 cells by qPCR: potential as diagnostic biomarker for rheumatoid arthritis. Rheumatology (Oxford). 2019;58(11):2015–24.
59. Georgiou KR, Scherer MA, King TJ, Foster BK, Xian CJ. Deregulation of the CXCL12/CXCR4 axis in methotrexate chemotherapy-induced damage and recovery of the bone marrow microenvironment. Int J Exp Pathol. 2012;93(2):104–14.
60. Cutler MJ, Lowthers EL, Richard CL, Hajducek DM, Spagnuolo PA, Blay J. Chemotherapeutic agents attenuate CXCL12-mediated migration of colon cancer cells by selecting for CXCR4-negative cells and increasing peptidase CD26. BMC Cancer. 2015;15:882.
61. Zhang M, Gao M, Chen J, Song L, Wei W. CP-25 exerts anti-angiogenic effects on a rat model of adjuvant-induced arthritis by promoting GRK2-induced downregulation of CXCR4-ERK1/2 signaling in endothelial cells. Mol Med Rep. 2019;20(6):4831–42.

Publisher's note